Modelling human immune response dynamics to Mycobacterium Tuberculosis infection

by

Kagiso Samuel Ramolotja

Thesis presented in partial fulfilment of the requirements for the degree of Master of Science in Mathematics in the Faculty of Science at Stellenbosch University

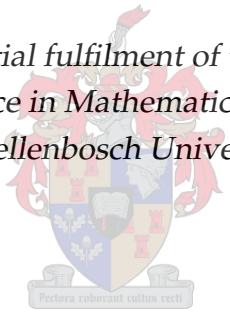

Department of Mathematical Sciences,
University of Stellenbosch,
Private Bag X1, Matieland 7602, South Africa.

Supervisor: Dr Gaston. K Mazandu & Co-supervisor: Prof. Farai Nyabadza

December 2017

Declaration

By submitting this thesis electronically, I declare that the entirety of the work contained therein is my own, original work, that I am the sole author thereof (save to the extent explicitly otherwise stated), that reproduction and publication thereof by Stellenbosch University will not infringe any third party rights and that I have not previously in its entirety or in part submitted it for obtaining any qualification.

Signature: Kagiso Samuel Ramolotja .....

Date: December 2017 .....

Abstract

Modelling human immune response dynamics to Mycobacterium Tuberculosis infection

Department of Mathematical Sciences,
University of Stellenbosch,
Private Bag X1, Matieland 7602, South Africa.

Thesis: MSc. (Mathematics)

December 2017

Tuberculosis (TB), caused by Mycobacterium tuberculosis (*MTB*) still poses a great challenge to the well-being of the population, particularly in Sub-Saharan Africa. The ability to trigger strong mounted cellular response within the host environment is daunting. The host cell depends on the robust adaptive cellular immunity to battle *MTB* infection. Of these, localizing TB bacteria by the development and the sustainability of a strong T helper type 0 cells (Th0) response is key to thwart *MTB* dissemination. The factors fuelling TB pathogenesis include, Human Immunodeficiency Virus (HIV) and TB co-pandemic, the growing burden of Multidrug-resistant TB (MDR-TB) and Extensive drug resistant TB (XDR-TB), and incompetency of host cell to kill *MTB*. The survived *MTB* load can trigger Latent TB infection (LTBI). In addition, the largely unknown biology of the host-*MTB* interaction, is yet to be elucidated. In this study, we develop a mathematical model capturing and addressing key dynamics of the adaptive host immune response to *MTB* infection. Of these, we consider the interplay of *MTB* with three distinct subsets of key immune cells and cell signalling molecules, namely; macrophages, T cells and cytokines. Furthermore, we explore the mechanisms of phagocytosis, T cells priming with delay, macrophage activation leading to lysis of infected cells. To estimate unknown parameters in the model, we perform curve fitting to experimental data of an infected mice using non-linear least square and Bayesian-based Markov Chain Monte

Carlo methods. We use the reproductive number $\mathfrak{R}_o$, to address factors altering the stability of the system. This study provides insight on how the immune system can be amplified to clear the survived intracellular *MTB*.

Keywords: Tuberculosis, granuloma, immune system, macrophages, cytokines, T cells, Mycobacterium tuberculosis.

Opsomming

Modellering van menslike immuunresponsdynamika vir Mycobacterium Tuberkulose infeksie

Departement Wiskundige Wetenskappe,
Universiteit van Stellenbosch,
Privaatsak X1, Matieland 7602, Suid Afrika.

Tesis: MSc. (Wiskunde)

Desember 2017

Tuberkulose (TB), wat veroorsaak word deur Mycobacterium tuberculosis (*MTB*), bied steeds 'n groot uitdaging tot die welvaart van die bevolking, spesifiek in Sub-Sahara Afrika. Die vermoë om 'n sterk gemonteerde sellulêre reaksie in die gasheeromgewing te wek is ontmoedigend. Die gasheersel is afhanklik van die robuuste aanpasbare sellulêre immuniteit om *MTB* infeksie teen te veg. Van hierdie, is die lokalisering van TB bakterië deur die ontwikkeling en volhoubaarheid van sterk T helper tipe 0 selle (Th0) reaksie die sleutel om *MTB* verspreiding te stuit. Die faktore wat TB patogene aanhelp sluit in 'n Menslike Immuniteitsgebreksvirus (MIV) en TB mede-pandemie, die groeiende las van multidwelmbestande TB (MDR-TB) en uitgebreide dwelmbestande TB (XDR-TB), en die onvermoë van die gasheersel om *MTB* dood te maak. Die oorlewende *MTB* lading kan lei tot 'n latente TB infeksie (LTBI). Daarbenewens moet die grootliks onbekende biologie van die gasheer-*MTB* interaksie nog toegelig word. In hierdie studie ontwikkel ons 'n wiskundige model wat die sleuteldinamika van die aanpasbare gasheerimmuunreaksie tot *MTB* infeksie opvang en aanspreek. Uit hierdie beskou ons die interspel van *MTB* met drie verskillende deelversamelings van sleutel immuunselle en selseiningsmolekules, naamlik: makrofage, T selle en sitokiene. Verder verken ons die meganismes van fagositose, T-sel primering met vertraging, makrofage aktivering wat lei tot lise in besmette selle. Om onbekende parameters in die model te benader,

pas ons 'n kurwepassing toe op eksperimentele data van besmette muise en gebruik nie-lineêre kleinste kwadrate en Bayesies-gebaseerde Markov-ketting Monte Carlo metodes, onderskeidelik. Ons gebruik die voortplantingsgetal $\mathfrak{R}_o$ om die faktore wat die stabiliteit van die stelsel verander, aan te spreek. Hierdie studie gee insig oor hoe die immuunstelsel versterk kan word om die oorblywende intrasellulêre *MTB* te verwyder.

Sleutelwoorde: Tuberkulose, granuloom, immuunstelsel, makrofage, sitokiene, T selle, Mycobacterium tuberculosis.

Acknowledgements

I would like to express my sincere gratitude to my supervisor Gaston K. Mazandu for his constructive comments, guidance, patience and motivation that contributed to the completion of this project. In addition, I would like to appreciate the constructive guidance, comments and suggestion from my co-supervisor Farai Nyabadza.

My appreciation to my colleagues at the Department of Mathematical Sciences. You have been a helping hand during hard times in the journey of my project. A special thanks to the staff members at Stellenbosch University for availing the facilities which helped me to complete my project.

On the other hand, my sincere gratitude to SACEMA for the financial support and monitoring of my progress, which ensured that I successfully complete my project. In addition, I would like to thank the SACEMA family for sharing with me their research experience which greatly enhanced my research skills.

Lastly, I would like to thank my family and friends for their continuous courage, support and guidance throughout this toughest journey. My gratitude to my friend Dikgale who continues to be a pillar of strength in my life. A special thanks to my mother and aunt for their maternal support.

Dedications

I dedicate this project to my grand mother Ramoshoane Fredericah Ramokolo for the educational foundation she has set that shaped my life. I would also like to dedicate this project to my aunt, Makgadi Annah Ledwaba and my mother Ramolotja Paulinah Ramokone, may GOD grant you more in your future endeavours.

Contents

List of Figures

List of Tables

Chapter 1

Introduction

1.1 History of Tuberculosis (TB)

The primary evidence of Mycobacterium (*M.*) tuberculosis (*MTB*) in both human and animal was spinal Tuberculosis, was attributed to spine bones with holes observed in 8000 BC [1]. In those days, the origin and morphology of Tuberculosis (TB) were still to be elucidated. Richard Morton (1637-1698) and others disputed inheritance as the transmission mode of TB. Without biological evidence they strongly argued TB had three phases namely; early TB infection, reactivated TB and active TB and, could be contracted by exposure with the infected individuals [2]. The cause of the disease was undiscovered until Benjamin Marten (1704-1722) postulated that infection was caused by a living creature calledbacteria [1]. It was Robert Koch (1843-1910) who successfully extracted the tubercle bacilli and demonstrated that TB is characterised by two stages, primary and secondary disease, respectively [2]. To date, we still rely on Phillip Klenche (1813-1881) hypothesis of possibility that as few as 10% of infected individuals fail to stop the dissemination of the TB bacteria, leading to active TB [3].

In 1865, Jean Antoine Villemen demonstrated that Tuberculosis (TB) is an infectious (transmissible) disease [1]. However, the mechanism in which the discovered tubercle bacilli invade the immune system was still unknown. Of these, a committed german physicist and scientist, Robert Koch (1843-1910) was the first to successfully discover that TB is caused by *MTB* [2, 3]. This discovery brought to light the morphology of the tubercle agent, in both animals and humans [4]. Although the phenotype and pathogenesis of *MTB* were still unknown. Several authors approximated that *MTB* originated 15000-20000 years ago [38]. However, in-depth research on *MTB* strains from

East African led to strong evidence that TB bacteria is 2-3 million years old [38]. This evidence supports the concept of a ancestral strain, that it is the original agent of the modern pulmonary Tuberculosis, which contradicts the hypothetical claim that *MTB* species matured from *M. bovis, M. microti, M. canettii and M. africanum* [1, 2, 38], respectively. In addition, it was strongly believed *MTB* genus evolved from *M. bovis* by human consumption of unpasteurized milk [1], supporting the transmission mode from cattle to human [1, 3]. The knowledge of TB was evolving with years due to its devastating impact in public health. The first animal experiments and animal models were performed and analysed on rabbits and guinea pigs [39]. Although the models significantly paved ways for new developments, they were limited by the availability of data.

1.2 Epidemiology and drug tolerance of Mycobacterium Tuberculosis

After the discovery of the tubercle bacilli, the first peak of TB cases were observed in the Europe, during the 19th century [47]. However, the number of TB cases and mortality declined in the 20th century as a result of awareness due to the immense TB deaths. This improved public health intervention methods and the availability of TB front-line drugs composed of isoniazid, rifampin, pyrazinamide and ethambutol [90], significantly contributed to the decline of TB prevalence [38, 47]. Despite the challenge of drug-resistance TB, the current TB burden in Africa, is an existing evidence that TB is fuelled by socio-economic status and poverty [1, 41].

TB symptoms include coughing of blood, rapid weight-loss, chest pains and lack of appetite [30] and this is also the case for latent TB infection (LTBI), which is asymptotic with 10% chance of reactivating [40]. An insight of *MTB* anatomy and phenotype led to development of diagnostic tools. To date, skin test, sputum test, Interferon gamma release assays (IGRAs) and other test assays, are used to detect TB [31]. However, the accuracy and time efficacy of the diagnostic tools is a shortfall [31]. We still lack rational and sensitive diagnostic tools that can quickly and efficiently detect TB [5], and also LTBI. The sputum test can cause false positives, i.e., failing to detect *MTB* load inside a sputum [31]. In vivo, this leads to untracked TB growth, and causing infected individuals to be highly infectious [43]. However, with the new advanced technologies, several diagnostic tools are still on the clinical trials [45]. Of these, some diagnostic tools are limited to the nature of TB. For instance, the Nucleic acid amplification tests (NATs) are limited to only detection of pulmonary Tuberculosis (PTB). In fact, it can be used to confirm the

results from sputum tests [45]. The new Line-probe assays is well-developed to extract co-ordinates, that are used to detect phenotypes of *MTB* that are able to trigger drug tolerant *MTB* [4, 33, 45]. However, these tools are only available in developed countries such as United States of America (USA), Germany and Belgium [45]. The availability of these advanced TB assays in developing countries where TB remains widespread is a necessity.

It took about 13 years (1908-1921) for the discovery [1] by french scientists Albert Calmette and Camille Guerin, the currently used TB vaccine, Bacillus Calmette Guerin (BCG) [1]. Despite the availability of this vaccine, the effectiveness and efficacy of the vaccine remain debatable. TB persistence in terms of prevalence and incidence is of great public health concern. Currently, factors fuelling epidemic burden, includes socio-economic, poverty, heterogeneity within individuals [4] and TB treatment time constraint [5].

There is a growing challenge of drug-tolerance, particularly extensively drug resistant TB (XDR-TB) [30], arising when resistant to second line drugs occur on top of multi drug resistant TB (MDR-TB) [32]. The phenotype of the *MTB* is a key factor in determining the immune tolerance and dissemination of the bacteria. The observation from real time tracking in both human and animal models revealed interesting characteristics of tuberculous bacilli. Its ability to switch avirulent phenotype, pose a challenge in the drug development [5]. Recent laboratory observations by John Szumowski and others showed that non-replicating *MTB* can cause drug tolerance [23]. Of these, intracellular *MTB* within macrophages turn-on efflux pumps, the proteins inducing *MTB* drug tolerance [23]. The virulent *MTB* strain such as *H37Rv* have been shown to knock down the immune system faster [29, 33, 39]. This is validated by laboratory observations using animal models [39].

Africa has the highest global burdened of Human Immunodeficiency Virus (HIV) and TB co-infection of about 28% as reported by the World Health Organisation (WHO) in 2014 [40]. TB persistence is intensively fuelled by drug resistance and co-infection (HIV and TB) with an excessive 50 % risk of TB recrudescence [40, 43, 44]. In South Africa (SA), despite the wide availability of TB front-line drugs, SA is still highly burdened with a growing challenge of drug tolerance TB [40]. The WHO has made significant contribution in the control of TB, highlighting key future research areas to be resumed. However, multi-drug resistant TB makes this pathogen the most lethal bacteria than it

was in the pre-antibiotic era [37]. It is clear that mutant TB has evolved strategies to survive intra-cellular anti-microbial attacks by the host cell. Understanding the biology of the *MTB* infection can be a steppingstone in restricting the pathogenesis of the *MTB*.

1.3 Immunology of Tuberculosis (TB)

TB is an aerosol infection on several parts of the organs, its ideal site is mainly lung tissues, resulting in pulmonary TB [5]. It is still unclear whether the lung is a pleasant habitat for *MTB*. The rationale is likely to be its ability to manipulate host system and survive in the lymph tissues [15]. Of these, the transmission dynamics are unique, compared to other leading infectious diseases. As few as 1-5 bacteria from a single droplet is sufficient to cause an infection [6]. This is specific to *MTB* since most infectious diseases require more than 1000 bacteria [6], or even more to initiate infection. Studies in rabbits which provided insights associated with the transmission dynamics of *MTB*, showed that fewer *MTB* load led to infection [24]. This mechanism supports the notion that tuberculous bacteria are unable to regulate the immune system [37], whereas most of the *MTB* will trigger the immune response which can effectively contain the *MTB* infection at the innate immunity [34, 36].

MTB infection requires a robust acquired cellular response. Although molecular and tissue scales are also important in controlling *MTB* infection. The cellular response to *MTB* infection have been shown to be the determinant in the disease outcome. Interestingly, the immune system can halt the activeness and dissemination of *MTB*. However, clearing *MTB* antigens is laborious due to the ability of the *MTB* to switch from replicative (growth) to non-replicative (dormancy) states [91]. The way in which the acquired response is expressed when primed by immune cells is critical for an competent immune system.

The regulation of both the innate and adaptive immunity remain controversial. There is a critical relation between the two immune responses, that still needs to be clearly described. During the early stages of *MTB* infection, macrophages receive signals from dendritic cells to locate and engulf the bacteria [37] to perform phagocytes [69]. However, the pathogen is able to evade this process [65]. In a study conducted in 2001 [65], it was observed that during the innate immunity, the hydrogen peroxide (oxidizer) is used by murine macrophages as a weapon to annihilate mycobacterial activities. Specifically, to facilitate the process of ingesting and killing the *MTB* [65]. Furthermore,

intracellular *MTB* within macrophages deplete nitric oxide and nitrogen, secreted by Interferon-gamma (IFN-γ) and Tumor Necrosis Factor-alpha (TNF-α) [23, 65], respectively. A study in murine models showed that during phagolysosome fusion, *MTB* secrete ammonia, sulfatides and related glycolipids to survive under harmful acidic conditions, with potential of hydrogen (PH) value of approximately 5.0 [65]. In addition, the lack of lysosome synthesis possibly due to microbial ammonia was observed in mice macrophages afflicted by TB bacilli [65]. However, this phenomenon was not seen in mice macrophages that are not infected with TB [65].

The switching from innate to adaptive immunity is a resulting failure of non-specific (innate) immunity which may be caused by the phagocytosis collapse [15, 49, 65]. The adaptive immunity is a network containing cells, molecules, cytokines and chemokines. Of these, the activation, priming and functioning of the immune system are induced by the phenotype and perturbations of the *MTB* [26, 61]. The keystones of the adaptive immunity are primarily T-lymphocytes, particularly $CD4^+$ T cells. Although, in the past, T-lymphocytes were not recognized as key mediators in TB control [36]. Recent studies have shown that lymphocytes are crucial in controlling TB and other leading communicable and non-communicable diseases such as, HIV and Cancer [36].

The organization of cells at the site of *MTB* infection, to restrict and contain the bacteria from replicating is formed, called granuloma [15, 19, 20, 22]. The granuloma is comprised of macrophages, class 1 and 2 major histocompatibility complex (MHC) mediated T cells, antibody cells (B cells) and other immune cells [19, 65]. The potency of the adaptive immunity lies on the receptors from cells of the innate immunity. However, the key mode of protective immunity used to confer successfully cell immunity to contain *MTB* is mainly the granuloma [49]. The granuloma is facilitated by strong response of class 2 MHC $CD4^+$ T cells and $CD8^+$ restricted by MHC class 1 molecules [10, 25, 50]. However, there is little experimental data to verify the protective effects of $CD8^+$, which includes production of IFN-γ and lysis of infected macrophages were redundant [25, 62, 65]. This suggest that $CD4^+$ T cells are the long serving soldiers of the immunity against TB [65]. Indeed, HIV infection in human greatly depletes the $CD4^+$ T cells and this has been shown to exacerbate the chances of TB infection or reactivation [30, 65]. The dynamics of *MTB* at different stages are yet to be understood [65].

The potency of TNF-α in facilitating the stability and maintenance of the granuloma is well described by several study groups. At the granuloma stage, TNF-α controls

the movement and activities of chemokines and related receptors [23, 65]. This control by TNF-α ensures that effector cells and other cells are recruited to the granuloma site [44, 58, 65]. Interestingly, TNF-α down-regulates the receptor CCR5 involved in recruiting immature macrophages (monocytes) [58, 65]. This suggest that TNF-α is involved in the differentiation of monocytes to rested macrophages [58]. This might be one of the mechanism of stabilizing the granuloma, by ensuring the ideal density of rested macrophages are recruited to the granuloma.

It has been shown that *MTB* is able to inhibit the expression of MHC class 2 molecules by infected macrophages [49, 65]. This results in a delayed T cell priming and prolonged T cell response [65]. In fact, observations from human studies evince that *MTB* blocks T helper type 1 (Th1) cells [67]. Nonetheless, the ability of the pathogen to promote T helper type 2 (Th2) cells response does not implicate *MTB* persistence [65]. This observation is yet to be elucidated by considering the in host TB granuloma dynamics [65]. In addition, investigating the relation of Th1 and Th2 response can reveal potent dynamics of TB granuloma.

The Th2 type cytokine IL-10, is considered the *MTB* beneficiary cytokine [76]. Its ability to deactivate cells and inhibit several activities describe the default anti-inflammatory immune response [58, 76]. However, the ability of *MTB* to mediate IL-10 activities remains a hurdle. The pathogen has been observed to use IL-10 as a tool for stimulating T cells differentiation (Th0 to Th2) [50, 51]. The role of IL-10 in promoting IL-4 is still to be elucidated. In most human *MTB* infection, the IL-4 is not highly expressed and its key anti-inflammatory role remain controversial. The ability of the pathogen to mutate and become drug tolerant are all challenges to the immune system.

Both avirulent and virulent TB strains exhibit different modulating strategies, and induce different immune response mechanisms [36]. Lalita and colleagues observed that *MTB* pathogen use the granuloma as a survival tool, it employ the ESX-1 secretion system to recruit rested macrophages through manipulating host Matrix metallopeptidase 9 (MMP-9) secretion system [37]. This suffice to deduce *MTB* benefits more from the granuloma. Understanding of the host-pathogen environment is crucial to identify factors that make *MTB* conquers the host response, and also identify elements within the immune system which can be targeted and amplified by the vaccine.

1.4 Problem statement

Tuberculosis remain one of the epicentre of public health, globally. Deaths due to TB were estimated to be 1.7 million annually in 2015 [71]. Approximating the number of TB deaths in the presence of HIV infection, can provide daunting insight of the expected number of TB deaths. In addition, the low risk of 5 - 10% is misleading [30, 38, 40], when considering the challenge of 15% TB adults risk and the stumbling block of XDR-TB. This XDR-TB alleviate the ability of the host to significantly prevent TB persistence. The TB granuloma is a structure used by the immune system to combat and prevent TB bacteria from spreading [71]. The emerging evidence suggests the granuloma benefits both the host cell and pathogen [28]. Triggering of this balance possibly due to aging or depletion of key cells, such as TNF-α, can result in reactivation of TB [75]. Additionally, the stimulation of bacterial protein, resuscitation promoting factor (*Rpf*), prompt TB re-activation [78].

MTB pathogenesis is aggravated by the largely unknown host-pathogen dynamics. We are faced with a challenge of both human and pathogen evolving, leading to complexity in screening host-pathogen interactions [59, 65, 77]. In addition, the biology of the granuloma from literature ignores different mechanisms used by *MTB* to circumvent strong cellular response [69]. The study of host-*MTB* interaction is given little attention, when considering the research on the immunology of TB. In fact, the dynamics of cellular response to *MTB* infection at the granuloma stage are not completely understood. In addition, most models were aimed at elucidating dynamics of infectious diseases at a population scale, see for instance [75]. As such, there are little efforts and very few mathematical approaches to understand the cellular dynamics of active TB and LTBI, respectively. Understanding host cell-*MTB* interaction can sharpen our insight into different stages of TB, and provide basis for drug and vaccine development that will yield long lasting immunity [75, 77].

In this study, we mathematically analyse and describe potent *MTB* infection dynamics at a cellular scale. In addition, we describe the interplay of both pro-inflammatory and anti-inflammatory cells and predict candidate immune cell biomarkers for potential protective immunity and vaccine development.

1.5 Motivation

Tuberculosis bacilli has proven to be the smartest bacteria in the history of infectious diseases, with its mechanisms to evade a strongly mounted immune system [36, 43]. The latter survived tuberculous bacilli leads to LTBI [44], with 90% chance of non-reactivation of TB. The remaining 10% re-activates. Moreover, TB cases are fuelled by an emerging challenge of drug tolerance and undiagnosed TB positive (TB^+) patients [40], toughening the advancement of TB control. In 2000, World Health Organization (WHO) aimed at reaching 70% of TB case detection rates and 85% treated rates of pulmonary TB [40]. This highlights of unachieved targets set by WHO is disturbing. In 2015, globally, the estimated prevalence of TB was 42% and decline of 1.5% annual average incidence was reported in 2015 [40]. Since only 63% of 9.6 million people estimated to be TB^+ were detected and tested [40]. The latter undiagnosed (37%) likely contribute to new infections that accelerate rising of TB [36, 40]. Of these, in 2014, deaths due to TB were reported to be approximately 16% (11% HIV^- and 6% HIV^+) [40].

Table 1.1: Models relevant to understanding the immune response during TB [11].

Model category	Biology	Biological scale	Time scale	Length scale	Model type.
Lymph node models	Peptide-MHC binding	Molecular	10^{-1}-10^{2} s	10^{-9}-10^{-8} m	Statistical
	Antigen uptake and presentation by single APC	Molecular/single cell	10^{1}-10^{3} s	10^{-5} m	Deterministic, continuous (ODE)
	Priming of single T cell by APC	Molecular Multiple cells	10^{1}-10^{2} s	10^{-3}-10^{-2} m	Deterministic, continuous (ODE)
	Cell interactions and T cell priming in LN	Cell/Tissue	10^{4}-10^{5} s	10^{-3}-10^{-2} m	Stochastic, discrete (ABM)
Granuloma models	TNF secretion and binding by single cells	Single cell	1-10^{1} s	10^{-6} -10^{-5} m	Deterministic, continuous (ODE)
	TNF secretion and binding by cells in granuloma	Cell/Tissue	1-10^{1} s	10^{-3} -10^{-2} m	Deterministic, continuous (PDE)
	Cell interactions in the lung to form granuloma	Cell/Tissue	10^{2}-10^{3} s	10^{-3} m	Stochastic, discrete (ABM)
Lung models	Cell interactions in the lung	Tissue/Organ	1 day	10^{-1} m	Deterministic, continuous (ODE,PDE)
Lymphatic/organ model	LN to other organ models	Organ/Body	10^{5}-10^{6} s	10^{-2} -1 m	Deterministic (Two compartmental ODE systems)

Table 1.1 shows the models aimed at understanding cellular dynamics of *MTB* infection. The studies on host-*MTB* are limited due to the complexity, unavailability of data and inaccessibility of lung biopsy samples [46]. Furthermore, very few *MTB* proteomes have been extensively studied. Nonetheless, protein database sites such as STRING and mint, which can be accessed on `http://string-db.org/` and `http://mint.bio.uniroma2.it/`, respectively, can be a useful tool to explore other sets of *MTB* protein-protein functional interactions. Additionally, animal models, in particular, widely studied mouse and zebra-fish models, provide essential tools that can be integrated with hu-

man models, to amplify cells facilitating cellular response to *MTB* infection. Although both humans and animals have different cellular structure, integrating animal models to human models in understanding diseases, has been a growing success. The animal granuloma in vivo models are assumed to closely resemble human TB dynamics [46], since both animals and humans share some biological features and functioning. In addition, it has been shown that low and high TNF-α concentrations in mice is associated with TB progression [44, 46]. This mechanism was also observed in TB patients at Chris Hani Baragwanath hospital [87]. Patients with active TB had low and elevated TNF-α concentrations, respectively. We need to study and understand the host-pathogen interaction, to model how the *MTB* circumvent the robust host defence.

1.6 Objectives of the project

In this project,

(I) We model the host immune response dynamics to the reactivation of the *MTB* infection using differential equations to elucidate cellular response to *MTB* infection.

(II) We fit the model to the experimental data to estimate model parameters using both, non-linear least square (NLS) and Bayesian-based Markov Chain Monte Carlo (MCMC) methods, respectively.

(III) We investigate components of the immune system that promote *MTB* growth.

(IV) In addition, we explore and analyse factors destabilizing the functioning of host cells.

(V) We address potent immune cells that can be amplified for therapeutic design.

1.7 Project outline

In the previous chapter 1, we state the background of TB and addressed the epidemiology and drug tolerance of *MTB*. In addition, in Chapter 2, we elucidate novel approaches related to the immunology of TB and also, we review mathematical models related to the cellular response of *MTB* infection. In chapter 3, we develop a mathematical scheme to investigate the human immune response to *MTB* infection. In this Chapter 3, the biology of each model equation is described. In Chapter 3, we perform mathematical analysis, to inspect the stability of the model. In Chapter 4, we present the analysis and

results of the model, this include model fit, estimated parameters, fitted plots, numerical simulation and sensitivity analysis. In the last Chapter 5, we use obtained results to give recommendations and conclude the project.

Chapter 2

Literature Review

The fight to control and eradicate TB prevalence and incidence remains a hopeless battle. The recent statistics on TB attest to this, especially in Africa with an estimate of 31% TB prevalence. Moreover, Southern Africa has the highest proportion of HIV^{+} individuals of which , about 45% receive Isoniazid Preventive Therapy (IPT) as a preventive treatment for LTBI [40, 42]. Additionally, approximately 74% of HIV-TB co-infection cases occurs in Africa [42]. It is necessary to investigate the relationship between these two lethal infections that manifest and kill its host quickly. To achieve the goal of combating TB and finding biomarkers of TB that can be used for designing effective diagnostic tools and development of rational human TB immuno therapy, there is a need to elucidate and understand the interaction between humans and *MTB*. It is therefore important to study and acquire extensive knowledge on the functioning of the immune system at different scales.

The immune system is a well-built stable network of cells, including Bone-marrow cells (B cells), T lymphocytes cells (T cells), defense cells (macrophages), dendritic cells also known as agent presenting cells (APC), and others [35, 47]. The main role of the immune system is to fight against unrecognised foreign invaders, such as germs, viruses and other pathogens [35]. The macrophages are the first to encounter the foreign pathogens, priming and stimulating other cells to perform activities that will facilitate in clearing out invaders in the system [35, 37, 46]. The default mechanism of "how the immune system works" is relatively uncomplicated. However, the immune response and regulation is specific to a disease [35], which harden our ability to better understand the immune response to an infection. This is exacerbated by the complexity of phenotype of bacteria or viruses. Of these, *MTB* has shown to be a lethal bacterium, with 498 known

strains [48]. These *MTB* virulent and avirulent strains are able to thwart the process of phagosome, thus overcoming the host defense mechanism. The cell-mediated response to *MTB* is a keystone component of the immune system in response to *MTB*. The T cells are synthesized by APC or infected alveolar macrophages for differentiation, proliferation and release pro-inflammatory and anti-inflammatory cytokines [47]. To explore and comprehend literature on cell mediated response to *MTB*, we only examine the role and activities of cells involved in anti-*MTB* defense response.

2.1 T cells

The life process of T cells begin with thymus maturing to precursor T cells [60, 61]. Thereafter, both naive $CD4^+$ and $CD8^+$ circulate in the lymph gland to locate antigens [61]. In addition, the effector and memory T cells mature from the naive T cells, after receiving stimuli signals from distinct cells [61, 62].

$CD4^+$ T cells are very potent in controlling chronic infections, in both humans and animals [49]. Most of the T cells at the site of infection are the branch of $CD4^+$ T cells, called $CD69^+ (\sim 50\%)$ [65]. Alternatively, we have diverse population of T cells, $CD4^+$, which is comprised of T helper cells (i.e., Th0, Th1 and Th2) and Treg cells, $CD8^+$ or Natural Killer Cells and $\gamma\delta$ T cells, respectively. However, other subsets of T cells, except $CD4^+$, are redundant in protective immunity against life-threatening infections, such as cancer, HIV and TB [63]. An observation from mouse models showed $CD8^+$ is more efficient than $CD4^+$ in high bacterial load infection [49]. However, since TB is a result of low-aerosol infection [64], the potency of $CD8^+$ may be remarkable in high-aerosol infections [49], indicating that $CD4^+$ can be more effective against the *MTB* infection.

We review the potent and functions of $CD4^+$ in the key role of immunity against *MTB* infection. The majority of T cells response occurs at the adaptive immune system stage, after the *MTB* antigen-presentation [50]. These T helper cells have time delay of approximately 5 days before they can respond to signals for protection [36]. However, there are other auto immune T cells migrating to the site of infection without binding to DC [50]. These T cells are flexible to organize for the battlefield (granuloma) of any infection. Indeed, the deficiency of $CD4^+$ in mice affected with TB led to prevailed and expansion of *MTB*, merely due to unstable and not well-formed granuloma [49, 50].

The launching of the granuloma is classified into four aspects. initiation, accumulation,

effector and resolution [36, 49, 50], respectively. The accumulation and effector stages are critical for granuloma development [51]. In fact, $CD4^+$ relocates and recruit stimulus cells to the granuloma [51], during the accumulation stage. The dysfunctional of $CD4^+$ T cells can be attributed to several virus or pathogen infections. For instance, novel approaches have demonstrated that HIV and TB co-infection depletes $CD4^+$ T cells [50]. The deficiency of $CD4^+$ contribute to unmaintained and unstructured granuloma, increasing the risk of progressing to active TB.

There is very little research on how Naive T cells are induced and activated for protective immunity. Furthermore, the key mediator of Naive T cells activation are bacterial spread or APC [36]. We can strongly hypothesize *MTB* exerts an inhibitory activity to resist the function of the APC. This *MTB* likely switches phenotype to avirulent [26], which may suppress the immune response. Unfortunately, the battle against this presumed puzzle requires data and extensive experiments on cells with the ability to recall the *MTB* antigen, T memory cells [25, 50] and conventional T cells, which are able to effectively differentiate into distinct effector cells. In fact, they are the prime targets for cells to be amplified for remedy design.

The migration and movement of T cells require signals from chemokines and associated receptors. For Th1 and Th2, chemokines CXCL and CCL facilitate signal pathways [49], respectively. Intuitively, the impact of chemokines on granuloma function remain unclear. Recently, tumor necrosis factor-α (TNF-α) and C motif chemokine ligand 2 (CCL2) have been shown to promote chemokine productivity [52]. In addition, it has been revealed that CCL2 prematurely navigate macrophages to the infection site [43].

To date, we still lack human novel approaches that can efficiently address the immune response dynamics after the *MTB* infection with low bacterial load. In addition, the secretion of cytokines by T cells, during *MTB* infection is still not well understood. Of these, human novel approaches aimed at understanding the roles of cytokines from the *MTB* infection reactivation to the disease outcome with knowledge that T cells play a fundamental role in TB immunity. The interdependence of macrophages, cytokines and T cells are building blocks of the acquired immunity.

Herein below, we review and address literature on the potency of the cytokines, macrophages and T cells during *MTB* infection. In particular, we inspect the role IFN-γ, necrosis factor-α (TNF-α) and an array of interleukins; 2, 4, 10, and 12, respectively.

2.2 Cytokines

The biological dynamics occurring in LTBI is unclear and not well understood. We are yet to describe how different cytokines are triggered during different phases of *MTB* infection. The cytokines regulate and facilitate the processes of most of the cells of the immune system [65]. We review the collaboration of different protective roles of cytokines during both active and dormant *MTB*. In addition, we include findings on screening studies and experiments on both primate and non-primate models. We also review cytokines dynamics during the *MTB* infection, precisely, T cells dependent cytokines. Although, cellular response to *MTB* infection is comprised of different expressed cytokines, its efficacy and involvement in the protective immunity are unique.

Different in vivo studies [29] on host-pathogen interaction have enlightened our knowledge on cellular immunity against pathogenesis of TB. Recently, beads-based multiple tool revealed IL-17 is associated with early protective immunity [12]. Despite this observation, individuals afflicted by TB still develop granulamous lesion [12, 47, 54]. The validation of IL-17 potency is controversial, patients with active disease showed high elevations of IL-17 [12, 54]. In addition, it is largely unclear what transpires in the early stages of the infection.

The breakthrough of IFN-γ potency in *MTB* infection paved ways for advancement in diagnosing TB. The IGRA use IFN-γ samples to detect *MTB* antigens, such as ESAT-6 [15]. However, its limitation to detect and recognize other antigens of mutant *MTB* is not heartening. The protective roles of IFN-γ during *MTB* infection include cell activation and lysis of infected cells [55], respectively. In fact, it is the most expressed inflammatory cell during both active and dormant stages of *MTB* [54]. Additionally, observations on mice showed that IL-12 is key to control *MTB* infection. Indeed, the cytokine proliferation induces IFN-γ for macrophage activation and apoptosis [51].

In most models, trial and error method is used to elect candidate cytokines involved in termination of cells. Recently, the IL-2 has been shown to effectively mediate killing of infected cells after the process of macrophage activation [12]. However, *MTB* block phagocytosis or phagolysosome intra-cellularly by manipulating the function of IL-10. Furthermore, at the granuloma stage, IL-2 recruit macrophage and T cells to the site of infection [12].

The fundamental role of TNF-α in sustaining the granuloma is well described and experimentally observed [54]. A study from a Chinese population observed that TNF-α is a factor determinant of active tuberculosis outcome [66], supporting its role in the granuloma maintenance. The ability of *MTB* to influence IL-4 response to halt TNF-α pathways was noticed [54]. Nonetheless, it is not known which mechanism does *MTB* employ to impede crucial protective operations by IL-4.
The interplay between IL-10 and *MTB* has been extensively analysed by several authors [65, 76]. Murine models continue to be fundamental in understanding key roles of IL-10, since human and murine share approximately 80% of IL-10 gene structure [55]. Furthermore, patients with lung TB secreted substantial amount of IL-10 and TGF-β [55], and this was also observed in cancer patients [58]. In both cancer and TB, IL-10 and TGF-β block T cells proliferation and deactivate macrophages [55].

The relevance of approaches demonstrating that IL-10 inhibition prevents disease severity is still to be clearly described. The in vivo mice model was used to examine the efficacy of BCG vaccine and this efficacy was achieved after blockage of IL-10 [55]. In addition, although different *MTB* strains manifest host immunity differently, IL-10 is a prime target used by most extensively studied *MTB* strains [28]. Despite various harmful activities of IL-10, there is no amplification of IL-10 from the current BCG vaccine.

2.3 Macrophages

Monocytes are released from the bone marrow to mature into alveolar macrophages [17]. In Greek language, "macro" symbolize larger and "phage" denote eater [57]. The appellation suggests resident alveolar macrophages are the first defense cells to encounter *MTB* [55], depending on the site of infection. Of these, macrophages are the best inducer of effector cells and other T cells subsets [49, 50, 55].

The key determinant of intracellular *MTB* evasion lies in the continuous cross-talk between macrophages and other soldier cells [55]. Macrophages signalling with other cells is Toll-like receptors 2 (TLR-2) dependent [15, 29, 55], and this signal pathway can be affected by microbial activities [80]. The findings in [15], suggests the ESAT-6 protein manipulates the host protein , β_2 micro-globulin (β2M), in order to alter the operations of MHC 1 class dependent antigen presentation and proliferation by macrophages via IL-12 and phagocytosis [15]. In addition, β2M is crucial in the presentation of MHC 1 class associated viruses and bacteria [81].

The capacity of the pathogen to delay immune system processes, negatively impact the functioning of MHC 2 class molecules by macrophages [55], leading to untracked bacterial growth intra-cellularly [15, 29]. The macrophages can be distinguished according to their biological functions, such as polarization phenotypes [82, 83]. This involves rested macrophages, infected macrophages and activated macrophages [8], respectively.

Rested macrophages await to engulf bacterial load without any protective operation [36] and they have been shown to kill negligible *MTB* load. However, due to factors attributed to *MTB*, they lack enough stimuli from pro-inflammatory cytokines, possibly macrophage activator, IFN-γ. Moreover, strong evidence suggests rested macrophages are the reservoir for *MTB* growth due to their lack of cytotoxicity [37, 59, 69, 72]. *MTB* delays the process of macrophage activation by switching phenotype [47, 55].

The molecular dynamics of macrophages infected by *MTB*, remain our focal point in terms of understanding and boosting cellular response to TB. Despite the well known role of IFN-γ in macrophage activation, IFN-γ augment the MHC 2 class molecules levels in macrophages [55]. In addition, TNF-α has recently been recognized to activate macrophages within the granuloma [43, 44]. The various activities of IFN-γ and TNF-α are the rational of assigning specific cells specialized roles to avert adverse effects. The visual aid of this concept is the tissue damage caused by macrophages after killing cells. This suggest every cell is uniquely robust for a particular immune function.

IFN-γ activated macrophages are well recognized by T cells. Of these, IL-12 allows activated macrophages to signal for T cells differentiation [54, 55]. In contrast, *MTB* adapts to harsh conditions within macrophages and block transformation of phagosome to phagolysosomes [27, 29, 56]. This phenomenon benefits the pathogen to survive throughout host life time. Of these, other studies demonstrated the latter survived *MTB* after bursting of activated macrophages switch phenotype to avirulent to escape phagocytosis [29, 56, 86, 88].

IL-2 mediates killing of activated macrophages containing significant *MTB* load [15, 55]. The success of *MTB* lies in the survived *MTB* that is competent to reactivate the infection. The assumption of slim risk of *MTB*infection may not be relevant considering the array of emerging *MTB* strains.

Furthermore, experiments from both human and non-human models have been extensively reviewed with findings demonstrating *MTB* induces the matrix metallopeptidase 9 (MMP9) gene to recruit rested macrophages to the granuloma site [22]. In addition, factors contributing to granuloma expansion are bursting of activated macrophages and arrival of rested macrophages [21]

2.4 TB Granuloma models

The primary TB models were formulated in 1994 and 1996 [75, 79], respectively. This models paved ways for investigating and understanding the biology of the host-*MTB* interaction within the granuloma. In addition, utilizing human real time tracking devices as a basis for elucidating the biology molecular structure of the granuloma can enhance our knowledge of granuloma dynamics. Although most studies are limited to unknown biology, which is exacerbated by the current poor diagnostic tools and the complexity of the human genome [45, 54, 75]. Furthermore, advanced TB assays are expensive and not widely available to the poorest population, mostly affected by TB. The lack of resources, such as lung biopsy samples, makes granuloma models potent tools to study the biology of the *MTB* infection [46]. The granuloma holds the differentiation of the two phases of TB, namely, active disease and latent sub-clinical infection [54, 59]. For active disease, high inflammation or tissue damage and enhanced IL-10 secretion is recognized by different study groups [69]. In addition, how the different levels of Th2, in particular IL-2, contribute to *MTB* pathogenesis is still controversial. The early events post *MTB* infection are not well understood. This is a roadblock for identifying target cells to be amplified to kill *MTB* before it proliferates, after the failure of the innate immunity. In addition, switching time from innate to adaptive immunity is yet to be delineated.

The most widely studied TB models, used to simulate human TB granuloma are the guinea pig and mouse models [46], respectively. With the availability of uncostly resources, non-human models remain relevant. In addition, Agent Based model (ABM) capturing stochastic granuloma dynamics enlightened our understanding of cell migration and activities within the granuloma. This model considers interesting properties, including granuloma dimension, cells in the granuloma, time-frame of cell interactions, and signals received from cells in the granuloma [6]. Although other dynamics have not been incorporated, simulation of T cell trafficking (time delay) and Naive $CD4^+$ were performed [6]. The results suggested that T cell trafficking was associated with high

bacterial burden [6]. In addition, with the enhanced host-pathogen interaction, simulation from ABM can be used to describe host cell components triggered for clearing *MTB* load. The ABM showed stable granuloma is maintained by $CD4^+$ T cells, possible by employing TNF-α [6, 23]. Additionally, TNF-α dependent macrophage activation is not efficient compared to IFN-α [6, 18]. Furthermore, there is a growing evidence suggesting low levels of IL-10 correlate with TB containment [8, 11]. This mechanism was validated by experimental studies [76].

Janis et al described factors attributed to cell dysfunction, and how TB latency is reached [14]. In addition, the cytotoxic cells and *MTB* evasion strategies were considered to be the rationale for cell dysfunction [12, 14]. The deficiency of IL-12 was associated with poor functioning of Th1 and Th2 [14], respectively. Of these, several cytokines were considered discriminants of LTBI and active TB, namely. IL-12, IFN-γ and IL-10 [14]. This findings were validated by the present experiments.

Lalita and colleagues used experiment from the zebrafish model to explore intriguing TB granuloma dynamics [29]; in particular, the pathogenesis of *MTB* at the granuloma stage [29]. Intuitively, intra-cellular life was analysed in accordance to how it switches anatomy to evade anti-microbial molecules [29, 46]. Furthermore, it was delineated how the granuloma benefit the bacteria more than the host [46, 59]. In addition, the factor altering granuloma growth include, *MTB* dependent macrophage recruitment [29] and infection of this recruited macrophages.

The summary in Table 2.1, shows the various TB approaches to understanding the human TB granuloma. Magombedze and Mulder reviewed and highlighted limitations and key advancement in mathematics and computational modelling of host-*MTB* interaction [75]. In summary, most studies are restrained by the complexity of the interaction between the host cell and the pathogen, which is fuelled by either the mutant *MTB* or drug resistant *MTB*.

Table 2.1: Granuloma models [75].

Latency/ Dormancy model (in vivo)	**Advantages**	**Disadvantages**.
Wayne model	Can simulate different non-replicating states of *MTB*. Cheap and flexible to use.	Limited to Hypoxia
Multi-stress model	Can be used to discriminate between active *MTB* and dormant *MTB*	Not easy to link with the biology of latency (in vitro)
Cornell model (in vitro)	Contains many immunological tools	Latency results do not correlate with the human LTBI dynamics.
Guinea pig/rabbit model	Show necrosis and granuloma structure similar to humans	Cannot explain the LTBI in humans.
Non-human primate model	Explain the dynamics of both active TB and LTBI in humans	Expensive and the challenge of ethical concerns.

To achieve global TB control, we need to review and investigate cell immunity to *MTB* and comprehend various cells produced at different phases of TB. In addition, we need to consider the variation between species, which may enhance the integration of diverse experimental data from different species [75]. Understanding the functions of key cells can aid in identifying the host-pathogen cell targets for potential TB vaccine and drug development to improve TB control.

Chapter 3

Tuberculosis micro-environment dynamics model

3.1 Model description

We develop a mathematical model that capture the interplay between three subsets of the T lymphocytes (CD4+), namely. T helper type 0 (T_0), T helper type 1 (T_1) and T helper type 2 (T_2). These T cells are sensitised by infected macrophages for macrophage activation, proliferation and other functions of protective immunity. In addition, we inspect three classes of macrophages, namely, rested macrophages (M_r),
infected macrophages (M_i) and activated macrophages (M_a) that interact within the host environment. The signalling and inflammatory movement of this macrophages are facilitated by chemokines and cytokines. For this study, we only examine the movement of cytokines of the type interleukin (IL) types 2, 4, 10 and 12, denoted by I_2, I_4, I_{10} and I_{12}, respectively. Additionally, we explore distinct roles of tumor necrosis factor-α (I_α) and interferon-γ (I_γ) in host protection against *MTB* infection.

M_r uptake the extracellular bacterial load (B), to perform phagocytosis. Of these, M_i perform the antigen presenting cells prompting T cells and other immune cells for cellular response against *MTB* infection [28]. We assume the released bacteria N, as a result of M_a reaching multiplicity of infection. Furthermore, the class of M_i and M_a contain intracellular bacteria. However, we only inspect the *MTB* to reproduce inside M_i at rate α_e. Of these, M_i uses α_{17} to induce T cell differentiation of both T_0 into T_1 and T_0 into T_2, respectively. Thereafter, the T helper type 1 secretes larger amounts of I_2, I_γ and I_α, for cell death, macrophage activation and stabilizing the host environment. We allow T-cell

proliferation by M_a.

To regulate this inflammatory processes, T_2 cells are stimulated after T_0 to T_2 differentiation for controlling inflammatory activities, producing regulatory cytokines I_4 and I_{10}. This regulatory cytokines down-regulate the immune system by preventing over-expression of cellular mediated immunity [10]. To investigate the balance between pro-inflammatory and anti-inflammatory cellular responses controlled by regulatory T (Treg) cell density, we inspect the capacity α_{treg} of I_{10} to promote T_2 response. In addition, we examine the capacity $(1 - \alpha_{treg})$ of I_{10} to inhibit T_1 response. Furthermore, we observe this capacity affects T cell priming by M_i. The time delay π_t is included to investigate its effect on T cell differentiation.

Since the cytotoxicity of $CD8^+$ T cells is inefficient in killing the *MTB* load [26]. We consider T_0 type cytokine I_2, to facilitate cell death of M_a. All the cells are considered to undergo programmed cell death or death due to aging. The ability to analyse the key cytokines I_γ and I_{10}, is crucial in the prevention of *MTB* persistence [76]. To capture and mathematically describe the dynamics in Figure 3.1, we translate this dynamics into a systems of differential equations below, taking into account the descriptions in the Table 3.1 and Table 3.2 below. In addition, the pro-inflammatory and anti-inflammatory cells dynamics are presented in Figure 3.2 and Figure 3.3, respectively.

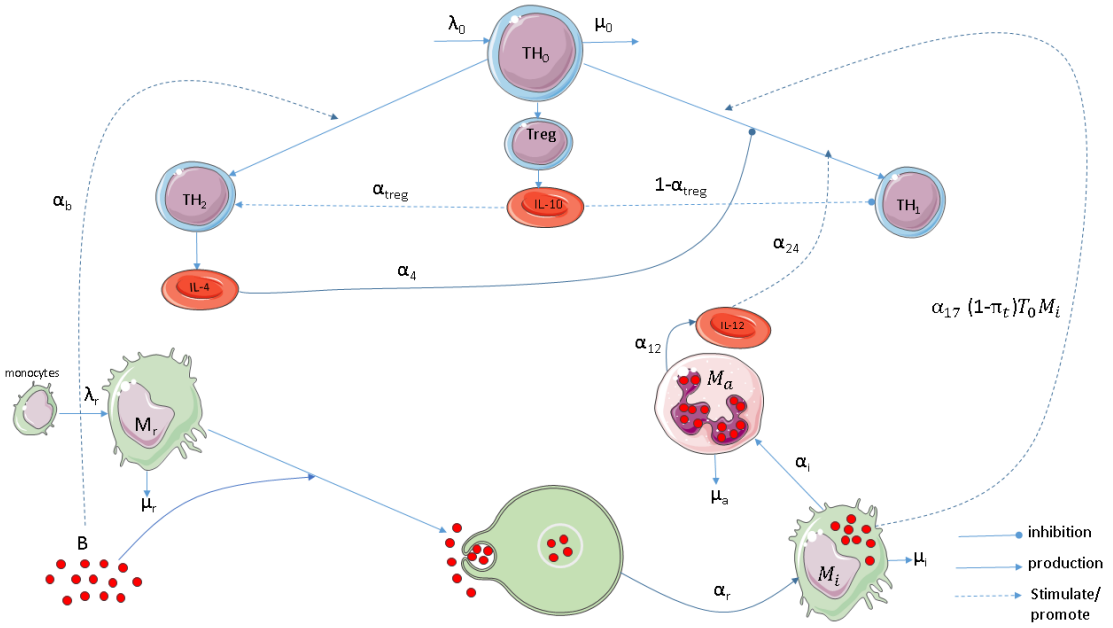

Figure 3.1: The diagram representing the cell to cell interaction of the protective immunity against *MTB* infection.

The associated model variables and parameters are listed in Table 3.1 and Table 3.2, respectively.

Table 3.1: Description of variables and their measurements.

Variable	Description	Units
M_r	density of rested macrophages	cells/ml
M_i	density of infected macrophages	cells/ml
M_a	density of activated macrophages	cells/ml
I_γ	concentration of interferon-gamma (IFN-γ)	pg/ml
I_2	concentration of interleukin-2 (IL-2)	pg/ml
I_4	concentration of interleukin-2 (IL-4)	pg/ml
I_α	concentration of tumor necrosis factor-α (TNF-α)	pg/ml
I_{10}	concentration of interleukin-10 (IL-10)	pg/ml
I_{12}	concentration of interleukin-12 (IL-12)	pg/ml
T_0	concentration of T-Helper Type 0 (Th0)	pg/ml
T_1	concentration of T-Helper Type 1 (Th1)	pg/ml
T_2	concentration of T-Helper Type 2 (Th2)	pg/ml
B	bacterial load of *MTB*	pg/ml

Table 3.2: Description of parameters and their units.

Parameter	Description	Units
λ_0	source of T_0	cells/ml/day
λ_r	source of resident macrophages from monocytes	cells/ml/day
α_4	inhibition rate of the I_α and M_a proliferation by I_4	pg/ cell day
α_{10}	the ability of the B to subvert I_{10} capacity	pg/ cell day
α_{12}	production rate of I_{12} by M_a	pg/ cell day
α_{13}	production rate of T_α by T_1	pg/cell day
α_{15}	production rate of I_4 by T_2	pg/cell day
α_{16}	production rate of I_2 by T_1	pg/cell day
α_{17}	priming rate of T_0 by M_i	ml/cell/day
α_{24}	proliferation rate by M_a	1/day
α_{25}	inhibition rate of I_γ response by I_{10}	1/day
α_b	priming rate of T_2 response by B	1/day
α_B	growth rate of B	1/day
α_i	macrophage activation rate for M_i due to I_γ	ml/cell/day
α_k	inhibition rate of I_{12} production by B using I_{10}	1/day
α_r	macrophage infection rate of M_i due to B	ml/cell/day
β_i	the capacity of M_i to reduce the bacterial load of B	cell^{-1}
β_{10}	the capacity of T_0 to differentiate	pg/ cell day
α_{treg}	the capacity of the I_{10} to promote T_2 response	pg/ cell day
$1-\alpha_{treg}$	the capacity of the I_{10} to inhibit T_1 response	pg/ cell day
μ_0	per capita death rate of T_0 due to apoptosis	1/day
μ_1	per capita death rate of T_1 due to apoptosis	1/day
μ_2	per capita death rate of T_2 due to apoptosis	1/day
μ_a	per capita death rate of M_a due to apoptosis	1/day
μ_g	per capita death rate of M_a due to bursting	1/day
μ_m	per capita death rate of M_a due to I_2	1/day
μ_i	per capita death rate of M_i due to apoptosis	1/day
μ_r	per capita death rate of M_r due to apoptosis	1/day
μ_B	per capita death rate of B	1/day
d_γ	degradation rate of I_γ	1/ day
d_2	degradation rate of I_2	1/ day
d_4	degradation rate of I_4	1/ day
d_α	degradation rate of T_α	1/day
d_{10}	degradation rate of I_{10}	1/ day
d_{12}	degradation rate of I_{12}	1/ day
π_t	time delay of T_0 priming by M_i	
N	multiplicity of infection (MOI) by M_a	

In the next section, we characterize the cells into pro-inflammatory and anti-inflammatory dynamics, and clearly define the equations that describe the cellular response to *MTB* infection.

3.2 Model development

3.2.1 Macrophages

We consider three distinct subsets of macrophages, namely rested macrophages, M_r, infected, M_i, and activated macrophages, M_a. Of these, the macrophage population is defined as $M = M_r + M_i + M_a$. M_r are macrophages waiting for chemokine signals to phagocyte the *MTB* load [20]. Many human and non-human models have demonstrated that M_r differentiate as a result of monocytes [17]. Moreover, M_r are one of the prime target of the extracellular bacteria, due to their inefficiency of cytotoxic activities [14]. Moreover, after M_r engulf B, they become infected thus moving from M_r into M_i [8].

T_1 secrete larger concentration of I_γ for activation of M_i, which become M_a [10]. Studies have shown that M_a can effectively eliminate other intracellular microbes [14, 21]. For *MTB*, it has been shown that M_a are potent in killing substantial *MTB* load [28]. We consider I_2 to activate and prepare M_a for cell death [20]. However, they are unable to clear the entire *MTB* load [27]. As a result, we include bi-fatality of M_a, death due to apoptosis and death due to bursting. Janis.E et al [14], strongly suggested T_1 response is down-regulated by several T_2 type cytokines, specifically, the frequently studied regulatory cytokine, I_{10} [22]. However, for M_a, we only consider I_4 to perform anti-inflammatory activities, merely blocking the process of proliferation. After phagolysosome collapse, M_a burst as a result of reaching maximal capacity of infection (MOI), leading to evasion of the intracellular *MTB* [9]. This released *MTB* by M_a is denoted by N.

Rested Macrophages (M_r)

The dynamics of M_r incorporates the mechanism of *MTB* uptake. This rested macrophages are differentiated from monocytes [17]. For this class of macrophages, we simply track the infection rate as a result of phagocytosis. The efficacy of the phagocytosis depends on the multiplicity of infection (MOI) [89] and the influence of toll-like receptors (TLR) signal pathway [88]. In addition, we consider the programmed cell death.

To formulate the equation for the rested macrophages, we represent the monocytes as the source λ_r, of rested macrophages M_r. Moreover, we denote the infection rate of M_r as α_r and the term $\alpha_r M_r B$ represent the normalized phagocytosis. So that the equation becomes,

$$\frac{dM_r}{dt} = \lambda_r - \alpha_r M_r B - \mu_r M_r. \tag{3.2.1}$$

Infected Macrophages (M_i)

After bacterial contagion M_r transform to class of infected macrophages (M_i). This class of macrophages prime T_0 for T_0 into T_1 differentiation. This leads to inducement of cytokines by T_1, including I_γ which prepare infected macrophages for apoptosis [10]. However, this process is down-regulated by the well-known anti-inflammatory cytokine I_{10} [76]. We assume no extracellular *MTB* release after the transformation from rested to infected macrophages, we only consider N, extracellular *MTB* after bursting of activated macrophages.

From the description above, we write the equation of M_i. Since the intracellular B within M_i is able to be dormant for a particular time [26]. We suppose M_i allows the B to replicate intra-cellularly. However, for the equation of M_i we only observe the priming of T cells with time delay, represented by the term $\alpha_{17}\pi_t M_i T_0$. Furthermore, M_i prime T cell differentiation at rate α_{17}, to be activated by I_γ at rate α_i. In addition, μ_i represent death rate due to apoptosis or aging [21], so that the equation of M_i becomes:

$$\frac{dM_i}{dt} = \alpha_r M_r B - \alpha_i M_i I_\gamma + \alpha_{17}\pi_t M_i T_0 - \mu_i M_i. \tag{3.2.2}$$

Activated Macrophages (M_a)

We present the class of activated macrophages, the key determinant of *MTB* dissemination. This class of macrophages arises from priming of T cells by M_i. This leads to inducement and triggering of the immune cells, such as the activation of M_i by interferon-γ. Furthermore, the M_a secrete I_{12} for T cell proliferation. This process promote the

killing efficacy of the I_2, the cytokine facilitating cell death. Moreover, over-expression of the immune response can provoke tissue damage or adverse reactions. Of these, the anti-inflammatory cytokines I_{10} and I_α prevent over-expression by blocking several activities [9, 20]. For M_a, the *MTB* bacteria manipulate I_{10} to block T cells proliferation by M_a.

To capture the dynamics of M_a, we consider key basic activities; bursting of M_a presented by $\mu_g M_a I_\alpha$. I_α is very effective in promoting distinct anti-mycobacterial activities including, macrophage and lymphocytes recruitment to achieve latency [21]. In this study, we consider I_α to facilitate the process of alleviating bursting of M_a. Additionally, we consider bi-fatality terms for M_a, death due to bursting of M_a, represented by μ_a, and the death μ_m administered by I_2. We deduce the concentration of M_a decrease as a result of performing the process of proliferation, explained by the term $\frac{\alpha_{12} M_a}{1+\alpha_k B I_{10}}$. It is assumed the population of B only increases inside the M_a, so that M_a equation becomes

$$\frac{dM_a}{dt} = \alpha_i M_i I_\gamma - \mu_a M_a - \mu_m M_a I_2 - \mu_g M_a I_\alpha - \frac{\alpha_{12} M_a}{1 + \alpha_k B I_{10}}. \tag{3.2.3}$$

3.2.2 T helper type 0 (Th0) cell (T_0)

T lymphocytes are well recognized as the mediators in cellular response to *MTB* infection and extraneous infectious diseases [15]. We have distinct array of T lymphocytes including $CD4^+$ and $CD8^+$, facilitating defence against infections and killing of infected cells [20], respectively. The T helper type 1 (Th1) and T helper type 2 (Th2) cells originate from undifferentiated Th0 with a source λ_0. Recently, the role of $CD8^+$ in performing cytotoxic activities in *MTB* infection, remains controversial. The LTBI phase exploit immune potent to efficiently kill and clear out the pathogen. Recent findings indicate *MTB* exhibits properties to survive phagolysosome fusion and granulysin [11]. Since it has been extensively studied that cytotoxic effects of $CD8^+$ are unable to clear the tuberculous bacilli [11]. As a result, we dont consider Cytotoxic T cells (CTL) from the $CD8^+$ T cells subsets performing granulysin or killing activity.

T_0 are synthesized by infected macrophages, through a process called T cell priming. This is a very crucial component of initiating host defence against *MTB* infection. It was hypothesized that intracellular *MTB* use the Toll-like receptors to interrupt both

the innate and adaptive immunity [50]. This mechanism includes manipulating the functioning of APC, which adversely affects switching from innate to adaptive immunity [74]. The roles T_0 can be categorized according to the pro-inflammatory and anti-inflammatory assignment. We described strategies employed by activated macrophages e to trigger T-cell mediated immunity.

T_0 originates from the thymus, naive T helper cells are then recruited to the site of infection to perform distinct anti-microbial duties [50]. We assume T cells have a source λ_0 from the naive T helper cells and die at rate μ_0. The fifth term represents T_0 proliferation that is induced by I_{12} at rate α_{24}. However, this process is regulated by I_4 at rate α_4. We include the priming term $\alpha_{17}M_iT_0$ without delay. However, we explore how the capacity of regulatory cytokine I_{10} to inhibit the differentiation of T_0 into T_1 influences the presentation of MTB by M_i. This is represented by the term $(1-\alpha_{treg})\beta_{10}M_iT_0$. Lastly, we denote, μ_0, death rate of T_0. Then we have,

$$\frac{dT_0}{dt} = \lambda_0 - \alpha_{17}M_iT_0 - \left(\alpha_{treg}\alpha_{10}BT_0\right) - (1-\alpha_{treg})\beta_{10}M_iT_0 - \frac{\alpha_{24}T_0I_{12}}{1+\alpha_4I_4} - \alpha_bBT_0 - \mu_0T_0. \tag{3.2.4}$$

3.2.3 Intracellular *MTB* (B)

We formulate and describe an equation explaining strategies used by MTB to trigger and elude the robust cellular response. The ability of the pathogen to colonize the host environment is a setback in the enhancement of the understanding of the MTB pathogenesis. After MTB infection, cultured filtrate proteins (CFP) including, ESAT-6 and Ag85B are the first MTB proteins to be recognized [74], this CFP escalates the complexity of the MTB pathogenesis. Of these, observation from mice models confirmed results of dead bacteria secreting proteins larger amounts of Ag85B protein [74]. The pathogenesis of MTB is greatly determined by the time efficacy of the immune response after aerosol infection with MTB [9, 50]. Specifically, late triggering of the innate immunity makes MTB disperse into other organs of the host [23] and blood stream for progression of active disease. To enrich our understanding of cell mediated response to MTB, we integrate these different interactions into the dynamics of MTB equation.

The bacterial load, B, which expound the disease outcome greatly depends on the growth rate. To capture this process, we consider the term α_eB. In the host-MTB battle, observations suggest MTB uses fatty acids and other lipids as a mechanism for survival [75]. Of

these, we consider them as the other source of emphMTB growth. Moreover, the term $\mu_g N M_a I_\alpha$ characterises the number of released bacteria, N, after bursting of M_a, which is due to the M_a reaching the maximal capacity of infection (MOI). This phenomenon is administered by I_α at the rate μ_g. Since we do not consider extracellular B, the term $\mu_g N M_a I_\alpha$ do not lead to new MTB infection. It only increase the bacterial load, B, that will be engulfed by M_r. The programmed cell death and the death due to the inability of the MTB pathogen to adapt the host environment is captured by the term $\mu_B B$. Then the equation of B is given by:

$$\frac{dB}{dt} = \alpha_e B + \beta_i M_i + \mu_g N M_a I_\alpha - \mu_B B. \tag{3.2.5}$$

3.2.4 Pro-inflammatory cells

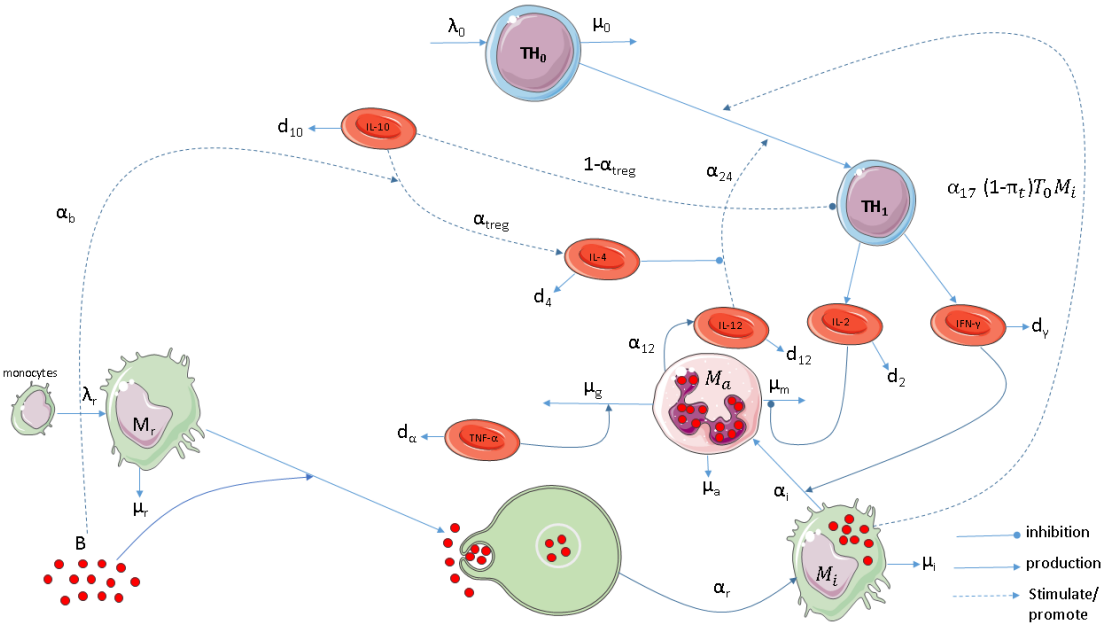

Figure 3.2: The pro-inflammatory cells.

The biology and formulation of the pro-inflammatory cell equations are elucidated below.

T helper type 1 (Th1) cell (T_1)

Th1 cells are the most important and effective subset of T_0 cells, which may facilitate pathology of viruses (i.e., HIV) and pathogens (i.e., *MTB*). The pathways in which distinct host cells are induced and expressed by different arrays of cells, is still to be elucidated. This hurdle is exacerbated by various factors, including how T cell response differs in early phase of the *MTB* infection and also in acute TB phase, respectively. Moreover, very few studies attempted to assimilate different experimental results. In this study, we inspect the key duties performed by T_1, during *MTB* infection. This may provide unrevealed pathways that may provide insights to the strong cellular immunity of *MTB*.

M_i are very useful in presenting *MTB* antigen prematurely before it manifests in the host domain [22]. Additionally, M_i are able to localize the pathogen and stimulate various immune cells. Thus, navigating the process of switching from innate to adaptive immunity [13, 25]. We suppose that all the presentation of *MTB* is administered by M_i.

We formulate the equation that explain the dynamics of T_1 over time. The term $\frac{\alpha_{24}T_0I_{12}}{1+\alpha_4I_4}$ represents the rate at which T_0 proliferate by interacting with I_{12}. This process is inhibited by I_4 at rate α_4. The term $\alpha_{17}(1-\pi_t)M_iT_0$ elucidate how time delay affect priming of T cells by M_i. In addition, we include the death term μ_1T_1. The remaining three terms tracks the production of pro-inflammatory cytokines ,I_γ, I_α and I_2 with the production rates given by α_1, α_{13} and α_{16}, respectively. However, this productions are down-regulated by regulatory cytokines I_4 and I_{10}. For I_α, we have high down regulation from both the regulatory cytokines. The inhibition rates are α_4 and α_{25}, respectively. For I_2 and I_γ, the inhibition rates are α_{11} and α_{25}, respectively. Then the equation becomes

$$\frac{dT_1}{dt} = \alpha_{17}(1-\pi_t)M_iT_0 - \frac{\alpha_1T_1}{1+\alpha_{25}I_{10}} - \frac{\alpha_{13}T_1}{1+\alpha_{25}I_{10}+\alpha_4I_4} - \frac{\alpha_{16}T_1}{1+\alpha_{25}I_{10}} + \frac{\alpha_{24}T_0I_{12}}{1+\alpha_4I_4} - \mu_1T_1. \tag{3.2.6}$$

3.2.5 Pro-inflammatory cytokines

The cytokines are very important type of proteins that are secreted by distinct cells of the immune cells. The interaction of cytokines with chemokines and T cells is vital for a stable and functional immune response to *MTB* and other infections [65, 76]. In this study, we consider Th1-type cytokines I_2, I_α and I_γ, respectively. In addition, anti-inflammatory activities will be performed by both T_2 and T_{reg} cell cytokines I_4 and I_{10}, respectively. Additionally, although I_2 plays a critical role in T-cell proliferation, elimi-

nating infected cells and also facilitating the movement of cell to cell interaction [10]. In this research, we observe its effect on preparing *MTB* infected cells to die.

The protective roles of I_γ and I_{10} have been well studied using both animal and human dummies [76, 84]. During early stages of TB, T_1 produces larger amounts of I_γ for macrophage activation [9]. Moreover, I_{10} regulate I_γ response to alleviate over-expression of the immune system [15]. Regulating on-going immune system is essential to counteract immuno-suppressive effects.

To analyse the dynamics of immune system, we introduce systems of non-linear differential equations, which includes production of specific cytokine by the associated cells and the depletion rates [16]. Although, cytokines are produced by distinct cells, the depletion and secretion solely rely on the phenotype of the cells prompting pertubations [16].

Interleukin-12 (I_{12})

I_{12} is secreted by M_a for T cell proliferation that stimulate T cell activation [10]. However, B manipulate I_{10} to halt this process [76]. We observe this mechanism at rate, α_{12}, and the inhibition rate α_k, the term $\alpha_k B I_{10}$ clearly illustrate this mechanism. Since cells undergo exhaustion , we include depletion term $d_{12} I_{12}$, so that:

$$\frac{dI_{12}}{dt} = \frac{\alpha_{12} M_a}{1 + \alpha_k B I_{10}} - d_{12} I_{12}. \tag{3.2.7}$$

Interleukin-2 (I_2)

I_2 is a vital Th1-type cytokine facilitating cell death and other biological functions [24]. In this study, we observe the effect of I_2 in preparing M_a for death at rate α_{16}. This process is down-regulated by the I_{10} at rate α_{25}, including the depletion rate d_2, the equation becomes,

$$\frac{dI_2}{dt} = \frac{\alpha_{16} T_1}{1 + \alpha_{25} I_{10}} - d_2 I_2. \tag{3.2.8}$$

Tumour Necrosis Factor-α (I_α)

I_α is essential for granuloma formation and for restraining the *MTB* dissemination [59, 66]. I_α has been extensively studied, enhanced I_α is associated with host resistance to *MTB* pathogenesis [22]. Studies on Mice with low-elevated I_α showed progression to fatal TB disease [14, 19]. Moreover, the observed patients with low concentration of I_α exhibited multibacillary lesions [23]. It remains unknown wherefore high and low elevated concentration contribute to progression to active TB.

This T_1 type cytokine, I_α, is produced by both lymphocytes and alveolar macrophages [23]. However, production by alveolar macrophages poses a challenge to host resistance to *MTB*, causing inflammation and tissue damage [20]. T_1 produces I_α to promote phagocytosis process in M_a and stabilize the granuloma. To alleviate inflammation, we incorporate both I_4 and I_{10} to regulate the I_α response at rates α_4 and α_{25}, respectively. Considering the production rate α_{13} and the depletion term $d_\alpha I_\alpha$. The equation becomes,

$$\frac{dI_\alpha}{dt} = \frac{\alpha_{13} T_1}{1 + \alpha_{25} I_{10} + \alpha_4 I_4} - d_\alpha I_\alpha. \tag{3.2.9}$$

Interferon-γ (I_γ)

Interferon-γ is significantly recognized to be a cornerstone cytokine in protection against intracellular pathogens, in particular *MTB* [22]. In addition, expression of I_γ in *MTB* infection is well investigated and addressed by different study groups [54, 62, 84]. However, little mechanisms are addressed on its potent at granuloma stage. I_γ potency was investigated during both active TB and LTBI [74]. For both, active TB and LTBI, I_α and I_γ were highly expressed in both active TB and LTBI [26, 28]. Moreover, the role of I_γ on macrophage activation is very crucial in preventing intracellular survival of *MTB* [9].

In this study, we observe how its production rate α_1 from T_1, which is inversely influenced by the concentrations of I_{10}. Thus, since I_{10} blocks T_1 response [76], we include

the inhibition rate α_{25} by I_{10}. Lastly, we have the depletion term $d_\gamma I_\gamma$, yielding to the equation below

$$\frac{dI_\gamma}{dt} = \frac{\alpha_1 T_1}{1 + \alpha_{25} I_{10}} - d_\gamma I_\gamma. \tag{3.2.10}$$

All of the rates with α indexes represent the production rate by a specific cell type and d_i denote the depletion of the cells.

3.2.6 Anti-inflammatory cells

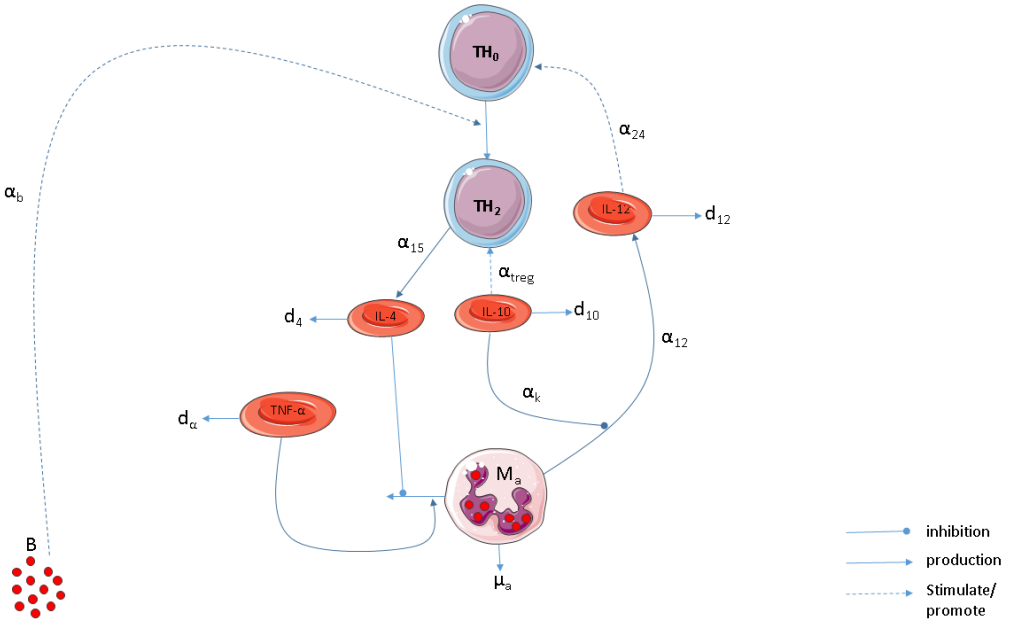

Figure 3.3: The anti-inflammatory cells.

T helper type 2 (Th2) cell (T_2)

We consider T_0 as the source of T_2, since it depends on the capacity of T_0 to differentiate. Furthermore, since B is able to exploit the T_2 response, we investigate how this activity impact cellular immunity of MTB. The formulation of T_2 equation is described below.

T_2 produces I_4 to perform distinct anti-inflammatory activities. This includes blockage of T_0 into T_1 differentiation and regulating the activities of both M_a and I_α. The term

$\alpha_b BT_0$ account for the mechanism in which *MTB* exhibit to promote differentiation from T_0 into T_2. We include the death term $\mu_2 T_2$. The equation of T_2 is given by

$$\frac{dT_2}{dt} = \alpha_b BT_0 - \alpha_{15} T_2 I_{10} - \mu_2 T_2. \tag{3.2.11}$$

3.2.7 Anti-inflammatory cytokine: Interleukin-4 (I_4)

The role of I_4 in *MTB* infection is debatable and still not clearly understood. Recently, I_4 has been appreciated to be T_2 type cytokine. Its expression during two phases of active TB and LTBI remain to be elucidated [27].
We use the fact that I_4 is secreted by T_2 and regulated by I_{10} with the depletion term $d_4 I_4$, including the production rate α_{15}, we have

$$\frac{dI_4}{dt} = \alpha_{15} T_2 I_{10} - d_4 I_4. \tag{3.2.12}$$

3.2.8 Regulatory cytokine: Interleukin-10 (I_{10})

I_{10} was first recognized and described as T_2 type cytokine, until extensive reviews from several authors disputed this findings [24]. Although distinct cells can produce it, recently, significant evidence suggest that Treg cells are the main producers of I_{10} [22]. However, its protective effects against TB remain unclear. It will be interesting to investigate unknown mechanisms of I_{10}. Since it is involved in many biological features of anti-inflammatory response. For this study, we observe its effects on halting and promoting several biological processes. This description is explained below.

We consider Treg cells as the producer with the depletion term $d_{10} I_{10}$. However, Treg cells are not included in our state variables. We consider the capacity α_{treg} of the I_{10} to promote T_2 response. The term $\alpha_{treg}\alpha_{10} BT_0$ represents the ability of the pathogen to subvert the capacity $0 \leq \alpha_{treg} \leq 1$ for I_{10}, to regulate T_0 response at rate α_{10}. In addition, we consider the capacity $(1 - \alpha_{treg})$ of I_{10} to inhibit T_1 response. The term $(1 - \alpha_{treg})\beta_{10} M_i T_0$ track how this capacity affects T cells priming. The parameter β_{10} delineates the capacity of T cells to differentiate after being primed by M_i. Then we have:

$$\frac{dI_{10}}{dt} = \alpha_{treg}\alpha_{10}BT_0 + (1-\alpha_{treg})\beta_{10}M_iT_0 - d_{10}I_{10}. \tag{3.2.13}$$

3.2.9 Mathematical representation of the model

The system of differential equations for the host immune cell-*MTB* dynamics are given by:

$$
\begin{cases}
\frac{dM_r}{dt} &= \lambda_r - \alpha_r M_r B - \mu_r M_r. \\
\frac{dM_i}{dt} &= \alpha_r M_r B - \alpha_i M_i I_\gamma + \alpha_{17}\pi_t M_i T_0 - \mu_i M_i. \\
\frac{dM_a}{dt} &= \alpha_i M_i I_\gamma - \mu_a M_a - \mu_m M_a I_2 - \mu_g M_a I_\alpha - \frac{\alpha_{12} M_a}{1+\alpha_k B I_{10}}. \\
\frac{dI_\gamma}{dt} &= \frac{\alpha_1 T_1}{1+\alpha_{25} I_{10}} - d_\gamma I_\gamma. \\
\frac{dI_2}{dt} &= \frac{\alpha_{16} T_1}{1+\alpha_{25} I_{10}} - d_2 I_2. \\
\frac{dI_4}{dt} &= \alpha_{15} T_2 I_{10} - d_4 I_4. \\
\frac{dI_\alpha}{dt} &= \frac{\alpha_{13} T_1}{1+\alpha_{25} I_{10}+\alpha_4 I_4} - d_\alpha I_\alpha. \\
\frac{dI_{10}}{dt} &= (\alpha_{treg}\alpha_{10} B T_0) + (1-\alpha_{treg})\beta_{10} M_i T_0 - d_{10} I_{10}. \\
\frac{dI_{12}}{dt} &= \frac{\alpha_{12} M_a}{1+\alpha_k B I_{10}} - d_{12} I_{12}. \\
\frac{dT_0}{dt} &= \lambda_0 - \alpha_{17} M_i T_0 - (\alpha_{treg}\alpha_{10} B T_0) - (1-\alpha_{treg})\beta_{10} M_i T_0 - \frac{\alpha_{24} T_0 I_{12}}{1+\alpha_4 I_4} - \alpha_b B T_0 - \mu_0 T_0. \\
\frac{dT_1}{dt} &= \alpha_{17}(1-\pi_t) M_i T_0 - \frac{\alpha_1 T_1}{1+\alpha_{25} I_{10}} - \frac{\alpha_{13} T_1}{1+\alpha_{25} I_{10}+\alpha_4 I_4} - \frac{\alpha_{16} T_1}{1+\alpha_{25} I_{10}} + \frac{\alpha_{24} T_0 I_{12}}{1+\alpha_4 I_4} - \mu_1 T_1. \\
\frac{dT_2}{dt} &= \alpha_b B T_0 - \alpha_{15} T_2 I_{10} - \mu_2 T_2. \\
\frac{dB}{dt} &= \alpha_e B + \beta_i M_i + \mu_g N M_a I_\alpha - \mu_B B.
\end{cases}
\tag{3.2.14}
$$

The initial conditions of the system in (3.2.14) are given by:

$M_r(0) = M_0, M_i(0) = 0, M_a(0) = 0, I_\gamma(0) = 0, I_2(0) = 0, I_4(0) = 0, I_\alpha(0) = 0, I_{10}(0) = 0,$
$I_{12}(0) = 0, T_0(0) = \tau_0, T_1(0) = 0, T_2(0) = 0, B(0) = B_0 \quad \text{with} \quad M_0 > 0, \tau_0 > 0 \quad \text{and}$
$B_0 \geq 0.$

To observe the host cell response to the initial *MTB* infection B_0. The behaviour of the system in (3.2.14) will be tracked over time.

3.3 Model analysis

The system of differential equations in (3.2.14) can be shortly written as the following initial value problem (IVP):

$$\begin{aligned} x'(t) &= f(t,x), \\ x(0) &= x_0, \end{aligned} \tag{3.3.1}$$

where

$$x(t) = \Big(M_r(t), M_i(t), M_a(t), I_2(t), I_4(t), I_{10}(t), I_{12}(t), I_\alpha(t), I_\gamma(t), T_0(t), T_1(t), T_2(t), B(t)\Big),$$
$$x_0 = (M_0, 0, 0, 0, 0, 0, 0, 0, 0, \tau_0, 0, 0, B_0)\,.$$

and

$$f : \mathbb{R}_+ \times \mathbb{R}_+^{13} \longrightarrow \mathbb{R}_+^{13}$$
$$(t,x) \longmapsto f(t,x) = (f_1, f_2, f_3, f_4, f_5, f_6, f_7, f_8, f_9, f_{10}, f_{11}, f_{12}, f_{13})\,.$$

with

$$\begin{aligned} f_1 &= \lambda_r - \alpha_r M_r B - \mu_r M_r. \\ f_2 &= \alpha_r M_r B - \alpha_i M_i I_\gamma + \alpha_{17}\pi_t M_i T_0 - \mu_i M_i. \\ f_3 &= \alpha_i M_i I_\gamma - \mu_a M_a - \mu_m M_a I_2 - \mu_g M_a I_\alpha - \frac{\alpha_{12} M_a}{1 + \alpha_k B I_{10}}. \\ f_4 &= \frac{\alpha_1 T_1}{1 + \alpha_{25} I_{10}} - d_\gamma I_\gamma. \\ f_5 &= \frac{\alpha_{16} T_1}{1 + \alpha_{25} I_{10}} - d_2 I_2. \\ f_6 &= \alpha_{15} T_2 I_{10} - d_4 I_4. \\ f_7 &= \frac{\alpha_{13} T_1}{1 + \alpha_{25} I_{10} + \alpha_4 I_4} - d_\alpha I_\alpha. \end{aligned}$$

$$f_8 = \left(\alpha_{treg}\alpha_{10}BT_0\right) + (1-\alpha_{treg})\beta_{10}M_iT_0 - d_{10}I_{10}.$$
$$f_9 = \frac{\alpha_{12}M_a}{1+\alpha_kBI_{10}} - d_{12}I_{12}.$$
$$f_{10} = \lambda_0 - \alpha_{17}M_iT_0 - \left(\alpha_{treg}\alpha_{10}BT_0\right) - (1-\alpha_{treg})\beta_{10}M_iT_0 - \frac{\alpha_{24}T_0I_{12}}{1+\alpha_4I_4} - \alpha_bBT_0 - \mu_0T_0.$$
$$f_{11} = \alpha_{17}(1-\pi_t)M_iT_0 - \frac{\alpha_1T_1}{1+\alpha_{25}I_{10}} - \frac{\alpha_{13}T_1}{1+\alpha_{25}I_{10}+\alpha_4I_4} - \frac{\alpha_{16}T_1}{1+\alpha_{25}I_{10}} + \frac{\alpha_{24}T_0I_{12}}{1+\alpha_4I_4} - \mu_1T_1.$$
$$f_{12} = \alpha_bBT_0 - \alpha_{15}T_2I_{10} - \mu_2T_2.$$
$$f_{13} = \alpha_eB + \beta_iM_i + \mu_gNM_aI_\alpha - \mu_BB.$$

Here we assume that x and f are non-negative functions, we are dealing with (cell) populations. Except explicitly expressed $x(t)$, is a set here for the rest of this thesis. Given U an open set of $\mathbb{R}^{n+1}$, we denote $C(U,\mathbb{R}^n)$, the set of continuous functions from U to I and $C^1(U,\mathbb{R}^n)$, the set of differentiable functions from U to $\mathbb{R}^n$. $C(I)$ and $C^1(I)$, for an interval $I \subset \mathbb{R}$, denote the set of continuous and derivable real-valued functions, respectively.

3.3.1 Existence and uniqueness to the problem (3.3)

Theorem 3.3.1. *IVP in (3.3) or (3.2.14) has a unique solution for all $t \in \mathbb{R}_+$, satisfying the initial condition $x(0) = x_0$.*

In fact, this is directly derived from the Picard Lindelöf theorem [94], which is stated as follows:

Theorem 3.3.2. *(Picard Lindelöf).*
Let $f \in C(U,\mathbb{R}^n)$ and consider the following IVP:

$$x'(t) = f(t,x),$$
$$x(t_0) = x_0,$$

if f is Lipschitz continuous in x and uniformly continuous in t, then the IVP above has a unique solution $x(t) \in C^1\left((t_0-\epsilon, t_0+\epsilon), \mathbb{R}^n\right)$, for some real value $\epsilon > 0$.

Note that for IVP in (3.3) and (3.2.14) $f \in C^1(\mathbb{R}_+ \times \mathbb{R}_+^{13}, \mathbb{R}_+^{13})$, i.e., f is differentiable, which implies that f is Lipschitz continuous in x and uniformly continuous with respect to t [94].

3.3.2 Positivity of solutions.

Lemma 3.3.3. *The following first order non-homogeneous linear equation:*

$$\begin{aligned} x'(t)+p(t)x(t) &= q(t), \\ x(t_0) &= x_0, \end{aligned} \tag{3.3.2}$$

where $p, q \in C((t_0-\epsilon, t_0+\epsilon))$ *for some real* $\epsilon > 0$, *has a unique solution for all* $t \in (t_0-\epsilon, t_0+\epsilon)$ *satisfying the initial condition* $x(t_0) = x_0$.

Let $F(t) = \int_{t_0}^{t} p(s)ds$. Multiplying (3.3.2) by $e^{F(t)}$ we obtain:

$$\frac{d}{dt}\left[e^{F(t)}x(t)\right] = e^{F(t)}q(t).$$

It follows that

$$e^{F(t)}x(t) = \int_{t_0}^{t} e^{F(s)}q(s)ds + x_0.$$

The solution is given by

$$x(t) = x_0 e^{-F(t)} + e^{-F(t)} \int_{t_0}^{t} e^{F(s)}q(s)ds.$$

It is worth noting that if $q(t) = 0$ for all t, then we obtain the first order homogeneous linear equation with solution $x(t) = x_0 e^{-F(t)}$.
We use the above Lemma 3.3.3 and initial conditions to show that regardless of cell deficiency or exhaustion, our system (3.2.14) remains positive for all time (i.e., $t \geq 0$).

Lemma 3.3.4. *In case of the* MTB *infection, all state variables in* (3.2.14) *are positive, i.e.,*

$$M_r(t) \geq 0, M_i(t) \geq 0, M_a(t) \geq 0, T_0(t) \geq 0, T_1(t) \geq 0, T_2(t) \geq 0 \quad \textit{and} \quad B(t) \geq 0$$

, then their solutions remain non-negative for all $t \geq 0$.

It is worth noting that for any living host, it is biologically rational to assume that $T_0(t) \geq 0$ and $M_r(t) \geq 0$. Here we show that biological rational still holds for the system (3.2.14). Furthermore, we are assuming the existence of the *MTB* infection, i.e., $B(t) \geq 0$, which may be 0 in case the host successfully clears the infection.
So, for the rested macrophages we have

$$\frac{dM_r}{dt} = \lambda_r - (\mu_r + \alpha_r B)\, M_r \geq -(\mu_r + \alpha_r B)\, M_r. \tag{3.3.3}$$

This implies that

$$\frac{dM_r}{M_r} \geq -(\mu_r + \alpha_r B)\, dt. \tag{3.3.4}$$

Then, we integrate the above equation (3.3.4) to obtain

$$\ln(M_r) = -\left(\mu_r t + \alpha_r \int_0^t B(s)ds\right) + C.$$

Which implies that

$$M_r(t) \geq M_r(0) e^{-\left(\mu_r t + \alpha_r \int_0^t B(s)ds\right)} \geq 0, \quad \text{since} \quad M_r(0) \geq 0.$$

Hence, $M_r(t)$ is always positive for all t.

Similarly for infected macrophages, we have that,

$$\frac{dM_i}{dt} \geq (\alpha_i I_\gamma(t) + \alpha_{17}\pi_t T_0(t) + \mu_i)\, M_i(t).$$

Dividing both sides by $M_i(t)$, we obtain

$$\frac{dM_i}{M_i} \geq (\alpha_{17}\pi_t T_0(t) - \alpha_i I_\gamma(t) - \mu_i)\, dt. \tag{3.3.5}$$

Integrating the above equation (3.3.5), we get

$$M_i(t) \geq M_i(0) e^{\left(\mu_i t + \alpha_i \int_0^t I_\gamma(s)ds - \alpha_{17}\pi_t \int_0^t T_0(s)ds\right)}$$

Since $M_i(0) \geq 0$ and $e^{\left(\mu_i t + \alpha_i \int_0^t I_\gamma(s)ds - \alpha_{17}\pi_t \int_0^t T_0(s)ds\right)} > 0$.

Therefore, $M_i(t)$ is always positive for all t.

For the activated macrophages, we have

$$M_a(t) = M_a(0) e^{-\left(\mu_a t + \mu_m \int_0^t I_2(s)ds + \mu_g \int_0^t I_\alpha(s)ds + \int_0^t K_0(s)ds\right)}.$$

Where

$$M_a(0) \geq 0 \quad \text{and} \quad K_0(t) = \frac{\alpha_{12}}{1 + \alpha_k B I_{10}}.$$

Thus, $M_a(t) \geq 0$ for all t.

Consider the following cytokine equation,

$$\frac{dI_\gamma}{dt} = \frac{\alpha_1 T_1}{1 + \alpha_{25} I_{10}} - d_\gamma I_\gamma \geq -d_\gamma I_\gamma.$$

$$I_\gamma(t) \geq I_\gamma(0) e^{-d_\gamma t} > 0, \quad \text{where} \quad I_\gamma(0) \geq 0.$$

Similarly, for the I_2 we have

$$I_2(t) \geq I_2(0) e^{-d_2 t} > 0, \quad \text{where} \quad I_2(0) \geq 0.$$

Furthermore, we integrate equations (3.2.7) and (3.2.9) to obtain,

$$I_{12}(t) \geq I_{12}(0)e^{-d_{12}t} > 0, \quad \text{where} \quad I_{12}(0) \geq 0.$$

Then for the I_α we have,

$$I_\alpha(t) \geq I_\alpha(0)e^{-d_\alpha t} > 0, \quad \text{where} \quad I_\alpha(0) \geq 0.$$

Then for the regulatory cytokines I_4 and I_{10} we integrate equations (3.2.12) and (3.2.13), to obtain

$$I_4(t) \geq I_4(0)e^{-d_4 t} > 0, \quad \text{where} \quad I_4(0) \geq 0.$$

For the I_{10}, we have

$$I_{10}(t) \geq I_{10}(0)e^{-d_{10}t} > 0, \quad \text{where} \quad I_{10}(0) \geq 0.$$

$$\frac{dT_0}{dt} = \lambda_0 - \alpha_{17}M_iT_0 - \left(\alpha_{treg}\alpha_{10}BT_0\right) - (1-\alpha_{treg})\beta_{10}M_iT_0 - \frac{\alpha_{24}T_0I_{12}}{1+\alpha_4I_4} - \alpha_bBT_0 - \mu_0T_0.$$

$$\geq -\left(\alpha_{17}M_i + \left(\alpha_{treg}\alpha_{10}B\right) + (1-\alpha_{treg})\beta_{10}M_i + \frac{\alpha_{24}I_{12}}{1+\alpha_4I_4} + \alpha_bB + \mu_0\right)T_0. \quad (3.3.6)$$

we simplify equation (3.3.6), such that

$$K_1(t) = \frac{\alpha_{24}I_{12}}{1+\alpha_4I_4}.$$

Thus, integrating equation (3.3.6), we obtain

$$T_0(t) \geq T_0(0)e^{-\left(\int_0^t M_i(s)ds\left[\alpha_{17}+\beta_{10}+\alpha_{treg}\beta_{10}\right]+\int_0^t B(s)ds\left[\alpha_{treg}\alpha_{10}+\alpha_b\right]+\int_0^t K_1(s)ds\right)} \geq 0.$$

Where

$$T_0(0) \geq 0$$

.

Hence, $T_0(t) \geq 0$ for all t.

For T_1, we consider the following inequality

$$\frac{dT_1}{dt} = \alpha_{17}(1-\pi_t)M_i T_0 - \frac{\alpha_1 T_1}{1+\alpha_{25}I_{10}} - \frac{\alpha_{13}T_1}{1+\alpha_{25}I_{10}+\alpha_4 I_4} - \frac{\alpha_{16}T_1}{1+\alpha_{25}I_{10}} + \frac{\alpha_{24}T_0 I_{12}}{1+\alpha_4 I_4} - \mu_1 T_1.$$

$$\geq -\left(K_2(t)+K_3(t)+K_4(t)+\mu_1\right)T_1. \tag{3.3.7}$$

Where

$$K_2(t) = \frac{\alpha_1}{1+\alpha_{25}I_{10}}, K_3(t) = \frac{\alpha_{13}}{1+\alpha_{25}I_{10}+\alpha_4 I_4}, \quad \text{and}$$

$$K_4(t) = \frac{\alpha_{16}}{1+\alpha_{25}I_{10}}.$$

Thus, the integration of equation (3.3.7) is given by

$$T_1(t) \geq T_1(0)e^{-\left(\int_0^t K_2(s)ds+\int_0^t K_3(s)ds+\int_0^t K_4(s)ds+\mu_1 t\right)} \geq 0.$$

Where

$$T_1(0) \geq 0$$

.

Therefore, $T_1(t)$ is always positive for all t.

For T_2, we consider the equation below

$$\frac{dT_2}{dt} = \alpha_b B T_0 - \alpha_{15}T_2 I_{10} - \mu_2 T_2.$$

$$\geq -\left(\alpha_{15}I_{10}(t)+\mu_2\right)T_2. \tag{3.3.8}$$

The integration of the above equation (3.3.8) is given by

$$T_2(t) \geq T_2(0)e^{-\left(\alpha_{15}\int_0^t I_{10}(s)ds+\mu_2 t\right)} \geq 0, \quad \text{where} \quad T_2(0) \geq 0.$$

Hence, $T_2(t)$ is always positive for all t.

Lastly, for the bacteria, B, we consider the equations below

$$\frac{dB}{dt} = \alpha_e B + \beta_i M_i + \mu_g N M_a I_\alpha - \mu_B B.$$

$$\geq -\left(\mu_B - \alpha_e\right) B \quad \text{positive} \quad \text{if} \quad \mu_B > \alpha_e. \tag{3.3.9}$$

Therefore, integrating the above equation (3.3.9), we obtain

$$B(t) \geq B(0)e^{-t(\mu_B-\alpha_e)} \geq 0, \quad \text{since} \quad B(0) \geq 0.$$

Thus, $B(t) \geq 0$ for all t.

Therefore, our state variables are all positive. This implies the solution of the system (3.2.14) will be non-negative for all $t \geq 0$.

Next, we want to show that all the state variables of the system of differential equations in (3.2.14) are bounded.

3.3.3 Feasible region

We now consider a positively invariant region, a set showing boundedness of the system (3.2.14). The set defined in lemma 3.3.2 with lower bound 0 and upper bound defined by macrophage, T cell and cytokine dynamics equations.

Lemma 3.3.5. *The set of solution of the system of differential equations in* (3.2.14) *is given by:*

$$\Omega = \Bigg\{ x(t) \in \mathbb{R}^{13}_{+} : M_r(t), M_i(t), M_a(t) \leq A; \\ I_\gamma(t) \leq F, I_2 \leq G, I_\alpha(t) \leq D, I_{12}(t) \leq H, I_4(t) \leq \xi, I_{10}(t) \leq \varphi; \\ T_0(t), T_1(t), T_2(t) \leq C; B(t) \leq E \Bigg\} \tag{3.3.10}$$

To show that all the solution originating in Ω, are restricted in the set Ω. We prove the unique boundedness of host cells equations in (3.2.14), according to the subsets, macrophages, T cells and cytokines, respectively.

We have shown in Lemma 3.3.2 that all states variables are positive. We now show that all the states variables of the system (3.2.14) are bounded, i.e., the set Ω is bounded.
To proceed, we first let

$$M = M_r + M_i + M_a$$

This implies that

$$\begin{aligned} \frac{dM}{dt} &= \frac{dM_r}{dt} + \frac{dM_i}{dt} + \frac{dM_a}{dt} \\ &= \lambda_r + \alpha_{17}\pi_t M_i T_0 - \mu_r M_r - \mu_i M_i - \mu_a M_a - \mu_m M_a I_2 - \mu_g M_a I_\alpha - \frac{\alpha_{12}}{1 + \alpha_k B I_{10}}. \\ &\leq \lambda_r - \mu_r M_r - \mu_i M_i - \mu_a M_a. \\ &\leq \lambda_r - \mu \left(M_r + M_i + M_a \right) \\ &\leq \lambda_r - uM. \end{aligned}$$

Where

$$\mu = min\{\mu_r, \mu_i, \mu_a\}$$

Integrating equation (3.3.3) with respect to t. We get that

$$M(t) \leq \frac{\lambda_r}{\mu} + \left(M(0) - \frac{\lambda_r}{\mu}\right) e^{-\mu t}.$$

We have that

$$\lim_{t\to\infty} \left(M(0) - \frac{\lambda_r}{\mu}\right) e^{-\mu t} \to 0.$$

Then we obtain,

$$M(t) \leq \frac{\lambda_r}{\mu} = A.$$

For the T cells, we first simplify below.

Setting $T = T_0 + T_1 + T_2$, we have:

$$\begin{aligned} \frac{dT}{dt} &= \frac{dT_0}{dt} + \frac{dT_1}{dt} + \frac{dT_2}{dt} \\ &\leq \lambda_0 - \mu_0 T_0 - \mu_1 T_1 - \mu_2 T_2 \\ &= \lambda_0 - \mu^* \left(T_0 + T_1 + T_2\right) \\ &= \lambda_0 - \mu^* T. \end{aligned} \tag{3.3.11}$$

With $\mu^* = \min\{\mu_0, \mu_1, \mu_2\}$.

Knowing that T is a positive function and integrating equation (3.3.11), we obtain:

$$0 \leq T(t) \leq \frac{\lambda_0}{\mu^*} + \left(T(0) - \frac{\lambda_0}{\mu^*}\right) e^{-\mu^* t}.$$

Therefore,

Finally

$$0 \leq T(t) \leq \frac{\lambda_0}{\mu^*} = C. \tag{3.3.12}$$

For the I_α, we know that

$$0 < \frac{1}{1 + \alpha_{25} I_{10+\alpha_4 I_4}} \leq 1,$$

which implies that.

$$\frac{dI_\alpha}{dt} \leq \alpha_{13} T_1(1) - d_\alpha I_\alpha.$$

Using the relation (3.3.3), it follows that

$$\frac{dI_\alpha}{dt} \leq \alpha_{13} C - d_\alpha I_\alpha.$$

Since I_α is a positive function of time and integrating each side of the inequality, we obtain:

$$0 \leq I_\alpha(t) \leq \frac{\alpha_{13} C}{d_\alpha} + \left(I_\alpha(0) - \frac{\alpha_{13} C}{d_\alpha} \right) e^{-d_\alpha t}.$$

Therefore

$$0 \leq I_\alpha(t) \leq \frac{\alpha_{13} C}{d_\alpha} = D.$$

For the bacteria, we have the equation below:

$$\frac{dB}{dt} = \alpha_e B + \beta_i M_i + \mu_g N M_a I_\alpha - \mu_B B.$$

Since $M(t) \leq A$ and $I_\alpha(t) \leq D$, we have:

$$\frac{dB}{dt} + (\mu_B - \alpha_e) B \leq (\mu_g ND + \beta_i) A. \tag{3.3.13}$$

Integrating equation (3.3.13) over the interval $[0, t)$ yield,

$$0 < B(t) \leq \frac{(\mu_g ND + \beta_i) A}{\mu_B - \alpha_e} + \left(B(0) - \frac{(\mu_g ND + \beta_i) A}{\mu_B - \alpha_e} \right) e^{-(\mu_B - \alpha_e)t}.$$

Taking the limit as t tends to infinity we have,

$$0 \leq B(t) \leq \lim_{t \to \infty} \left(\frac{(\mu_g ND + \beta_i) A}{\mu_B - \alpha_e} + \left(B(0) - \frac{(\mu_g ND + \beta_i) A}{\mu_B - \alpha_e} \right) e^{-(\mu_B - \alpha_e)t} \right).$$

Therefore, we get

$$0 \leq B(t) \leq \frac{(\mu_g ND + \beta_i) A}{\mu_B - \alpha_e} = E.$$

To show the boundedness of the cytokines. We first show that IL-10 is bounded. Consider the equation below,

$$\frac{dI_{10}}{dt} = \alpha_{treg} \alpha_{10} B T_0 + (1 - \alpha_{treg}) \beta_{10} M_i T_0 - d_{10} I_{10}. \tag{3.3.14}$$

We know that

$$M_i(t) \leq A, T_0(t) \leq C \quad \text{and} \quad B(t) \leq E. \tag{3.3.15}$$

After integrating equation (3.3.14) and considering the expressions in (3.3.15). We obtain:

$$0 \leq I_{10}(t) \leq \frac{\alpha_{treg}\alpha_{10}EC}{d_{10}} + \frac{\left(1-\alpha_{treg}\right)\beta_{10}AC}{d_{10}} + \left(I_{10}(0) - \frac{\alpha_{treg}\alpha_{10}EC}{d_{10}} + \frac{\left(1-\alpha_{treg}\right)\beta_{10}AC}{d_{10}}\right)e^{-d_{10}t}.$$

Applying the limit as $t \to \infty$, we notice that

$$\left(I_{10}(0) - \frac{\alpha_{treg}\alpha_{10}EC}{d_{10}} + \frac{\left(1-\alpha_{treg}\right)\beta_{10}AC}{d_{10}}\right)e^{-d_{10}t} \to 0 \quad \text{as} \quad t \to \infty.$$

Thus, the boundedness of IL-10 is given by:

$$\begin{aligned} 0 \leq I_{10}(t) &\leq \frac{\alpha_{treg}\alpha_{10}EC}{d_{10}} + \frac{\left(1-\alpha_{treg}\right)\beta_{10}AC}{d_{10}} \\ &= \varphi. \end{aligned}$$

We proceed by showing that IL-4 is bounded. Since we have proven that $B(t) \leq E$ and $I_{10} \leq \varphi$. The equation of IL-4 become,

$$\frac{dI_4}{dt} = \frac{\alpha_{15}E\varphi}{d_4} - d_4 I_4.$$

We have that

$$0 \leq I_4(t) \leq \frac{\alpha_{15}E\varphi}{d_4} + \left(I_4(0) - \frac{\alpha_{15}E\varphi}{d_4}\right).$$

It follows that

$$\lim_{t\to\infty} I_4(t) \leq \frac{\alpha_{15} E\varphi}{d_4} = \xi.$$

The boundedness of the pro-inflammatory cytokines, IFN-γ, IL-2 and IL-12 are shown by the expression below.

$$0 \leq \lim_{t\to\infty} I_\gamma(t) \leq \frac{\alpha_1 C}{d_\gamma\,(1+\alpha_{25}\varphi)} = F \quad \text{and}$$

$$0 \leq \lim_{t\to\infty} I_2(t) \leq \frac{\alpha_{16} C}{d_2\,(1+\alpha_{25}\varphi)} = G.$$

For the IL-12, we use $B(t) \leq E$, $M_a(t) \leq A$ and $I_{10} \leq \varphi$. We obtain,

$$\lim_{t\to\infty} I_{12}(t) \leq \frac{\alpha_{12} A}{d_{12}\,(1+\alpha_k \varphi E)} = H.$$

The feasible solutions sets of the macrophages, T cells, cytokines and bacteria are given by,

$$\begin{aligned}\Omega = \Big\{ & x(t) \in \mathbb{R}_+^{13} : M_r(t), M_i(t), M_a(t) \leq A; \\ & I_\gamma(t) \leq F, I_2 \leq G, I_\alpha(t) \leq D, I_{12}(t) \leq H, I_4(t) \leq \xi, I_{10}(t) \leq \varphi; \\ & T_0(t), T_1(t), T_2(t) \leq C; B(t) \leq E. \Big\}\end{aligned} \tag{3.3.16}$$

Where

$$
\begin{aligned}
A &= \frac{\lambda_r}{\mu}, \\
C &= \frac{\lambda_0}{\mu^*}, \\
D &= \frac{\alpha_{13} C}{d_\alpha}, \\
E &= \frac{\left(\mu_g N D + \beta_i\right) A}{\mu_B - \alpha_e}, \\
\varphi &= \frac{\alpha_{treg} \alpha_{10} E C}{d_{10}} + \frac{\left(1 - \alpha_{treg}\right) \beta_{10} A C}{d_{10}}, \\
\xi &= \frac{\alpha_{15} E \varphi}{d_4}, \\
F &= \frac{\alpha_1 C}{d_\gamma \left(1 + \alpha_{25} \varphi\right)}, \\
G &= \frac{\alpha_{16} C}{d_2 \left(1 + \alpha_{25} \varphi\right)}, \\
H &= \frac{\alpha_{12} A}{d_{12} \left(1 + \alpha_k \varphi E\right)}.
\end{aligned}
$$

Therefore, the system in (3.2.14) is bounded by the region Ω. And for all t positive, the solutions will remain in Ω.

3.3.4 *MTB* infection-free equilibrium point

Definition 3.3.6. *The* MTB *infection-free equilibria is a point where the bacteria is not present in the system [70].*

We now consider a state where the *MTB* load is cleared from the system (3.2.14). Since there is no *MTB* infection, $B(t) = 0$. This leads to the termination of processes, including uptake of the the bacteria and macrophage activation, respectively. This set the dynamics of the cells $M_i(t)$ and $M_a(t)$ to *MTB* free state, i.e., $M_i(t) = M_a(t) = 0$. We remain with the reduced system of $M_r(t)$ and $CD4^+$ T cells subsets, T_0, T_1, and T_2, respectively. This resulting subsets of equations are given by:

$$\begin{aligned}
\frac{dM_r}{dt} &= \lambda_r - \mu_r M_r. \\
\frac{dT_0}{dt} &= \lambda_0 - \mu_0 T_0. \\
\frac{dT_1}{dt} &= -(\alpha_1 + \alpha_{13} + \alpha_{16} + \mu_1) T_1. \\
\frac{dT_2}{dt} &= -\mu_2 T_2.
\end{aligned} \tag{3.3.17}$$

We now equate and solve the above system (3.3.4) to zero so that,

$$\begin{aligned}
\lambda_r - \mu_r M_r &= 0 \\
\lambda_0 - \mu_0 T_0 &= 0 \\
-(\alpha_1 + \alpha_{13} + \alpha_{16} + \mu_1) T_1 &= 0 \\
-\mu_2 T_2 &= 0
\end{aligned}$$

Which implies that $M_r = \frac{\lambda_r}{\mu_r}$ and $T_0 = \frac{\lambda_0}{\mu_0}$.

Thus, the *MTB* infection free equilibrium point is given by:

$$\Big(M_r(t), M_i(t), M_a(t), I_2(t), I_4(t), I_{10}(t), I_{12}(t), I_\alpha(t), I_\gamma(t), T_0(t), T_1(t), T_2(t), B(t)\Big)$$

$$\Rightarrow \beta_0 = \left(\frac{\lambda_r}{\mu_r}, 0, 0, 0, 0, 0, 0, 0, \frac{\lambda_0}{\mu_0}, 0, 0, 0\right)$$

From the above E_0, we can see the *MTB* infection free equilibrium (E_0) is maintained by both rested macrophages (M_r) and T helper type 0 cells (T_0). For M_r, the ratio $\frac{\lambda_r}{\mu_r}$ represents the proportions of the recruited rested macrophages to death rate. In addition, our system 3.2.14 solely rely on the T helper type 0 cell growth factor, $\frac{\lambda_0}{\mu_0}$. The existence of M_r and T_0 at E_0 shows that the model explains a state where the immune system is robust to detect and contain the new *MTB* infection.

3.3.5 Endemic equilibrium

We now consider a state where the *MTB* infection cannot be eradicated from the host. This can be regarded as a condition under which the host reach LTBI, which is an equilibrium or a state of non-replicating or dormant MTB [75]. To compute the endemic equilibrium, we employ R to set the system (3.2.14) to zero and solve for the state variables. This endemic equilibrium is given by the following vector:

$$E_1 = \left(M_r^*(t), M_i^*(t), M_a^*(t), I_2^*(t), I_4^*(t), I_{10}^*(t), I_{12}^*(t), I_\alpha^*(t), I_\gamma^*(t), T_0^*(t), T_1^*(t), T_2^*(t), B^*(t)\right)$$

such that

$$M_r^* = \frac{\lambda_r}{\alpha_r B^* + \mu_r}, M_i^* = \frac{\alpha_r M_r^* B^*}{\mu_i + \Psi_1 T_1^* + \alpha_{17}\pi_t T_0^*}, M_a^* = \frac{\alpha_{12}\left(1 + \frac{d_{10}}{B^* T_0^*\left(\Psi_3 - \Psi_4 M_i^*\right)}\right) - \Psi_1 M_i^* T_1^*}{\Psi_2 - \Psi_5 T_1^* - \mu_a},$$

$$I_2^* = \frac{\alpha_{16} T_1^*}{d_2\left(1 + \alpha_{25} I_{10}^*\right)}, I_4^* = \frac{\alpha_{15} T_2^* I_{10}^*}{d_4}, I_{10}^* = \frac{\alpha_{treg}\alpha_{10} B^* T_0^* + \left(1 - \alpha_{treg}\right)\beta_{10} M_i^* T_0^*}{d_{10}},$$

$$I_{12}^* = \frac{\alpha_{12} T_0^*}{d_{12}\left(1 + \alpha_k B^* I_{10}^*\right)}, I_\alpha^* = \frac{\alpha_{13} T_1^*}{d_\alpha\left(1 + \alpha_{25} I_{10}^* + \alpha_{18} I_4^*\right)}, I_\gamma^* = \frac{\alpha_1 T_1^*}{d_\alpha\left(1 + \alpha_{25} I_{10}^*\right)},$$

$$T_0^* = \frac{\lambda_0}{\mu_0 + \Psi_7 M_a^* + \left(\left(\alpha_b + \Psi_6\right) B^* + \left(\alpha_{17} - \Psi_4\right) M_i^*\right) + \alpha_b B^*},$$

$$T_1^* = \frac{\Psi_8 M_i^* T_0^* + \Psi_7 M_a^* T_0^*}{\mu_1 - \frac{\Psi_{10}}{1 + \Psi_9\left(\Psi_6 B^* T_0^* - \Psi_4 M_i^* T_0^*\right)}}, T_2^* = \alpha_b B^* T_0^* \mu_2 - \left(\Psi_6 B^* + \left(\beta_{10} - \Psi_{12} M_i^* T_0^*\right)\right)\Psi_{11},$$

$$B^* = \frac{\beta_i M_i^* + \Psi_5 M_a^* N T_1^*}{\mu_B - \alpha_e}.$$

Where

$$\Psi_1 = \frac{\alpha_i \alpha_1}{d_\gamma}, \Psi_2 = d_{10} d_{12}, \Psi_3 = \alpha_k \alpha_{10} \alpha_t, \Psi_4 = (-1 + \alpha_t)\, \beta_{10},$$
$$\Psi_5 = \frac{\alpha_{13} \mu_g}{d_\alpha}, \Psi_6 = \alpha_{10} \alpha_t, \Psi_7 = \frac{\alpha_{12} \alpha_{24}}{d_{12}}, \Psi_8 = (1 - \pi_t)\, \alpha_{17}, \Psi_9 = \frac{\alpha_{25}}{d_{10}},$$
$$\Psi_{10} = (\alpha_1 + \alpha_{13} + \alpha_{16}), \Psi_{11} = \alpha_{15} \beta_{10}, \Psi_{12} = \alpha_t \beta_{10}.$$

3.3.6 The basic reproduction number

Definition 3.3.7. *The reproduction number $\mathfrak{R}_o$, is the number of secondary infections caused in the population, by a single infected individual [52] at an infection free equilibrium.*

Experimental studies showed that each macrophage can engulf approximately 5 *MTB* load [86]. Of these, we incorporate this observation and define $\mathfrak{R}_o$ as the whole number of secondary infected macrophages (M_i), that is caused by about 5 *MTB* load [19, 20]. Here, we use the next generation method to compute the $\mathfrak{R}_o$.

Let

- $\mathcal{F}_c(x)$ denotes the rate of new infected macrophages M_i in the cell.
- $\mathcal{V}_c^+(x)$ denotes the rate at which *MTB* infection is transferred within a cell.
- $\mathcal{V}_c^-(x)$ denotes a cell able to transmit infection leaves the host system.

Therefore, the *MTB* infection system can be defined as,

$$\frac{dx_c}{dt} = \mathcal{F}_c(x) - \mathcal{V}_c(x). \tag{3.3.18}$$

Where $\mathcal{V}_c(x) = \mathcal{V}_c^+(x) - \mathcal{V}_c^-(x)$, and $c = \{1, \ldots, k\}$, are cells capable of infecting other cells. For the above system (3.3.18), it is assumed that $\mathcal{F}_c(x)$ and $\mathcal{V}_c(x)$ are both differentiable functions [70]. The extend of the system in (3.3.18) at *MTB* infection free state, E_0 is given by:

$$F = \left(\frac{\partial \mathcal{F}_c}{\partial x_j}(E_0)\right) \quad \text{and} \quad V = \left(\frac{\partial \mathcal{V}_c}{\partial x_j}(E_0),\right)$$

With $1 \leq c$ and $j \leq k$. We obtain $\Re_o$ from the eigenvalues of the resulting matrix FV^{-1}. Here, the reservoirs of MTB are B, M_a and M_i, respectively. The set of equations are given by:

$$\begin{aligned}
\frac{dB}{dt} &= \alpha_e B + \beta_i M_i + \mu_g N M_a I_\alpha - \mu_B B, \\
\frac{dM_i}{dt} &= \alpha_r M_r B - \alpha_i M_i I_\gamma + \alpha_{17} \pi_t M_i T_0 - \mu_i M_i, \\
\frac{dM_a}{dt} &= \alpha_i M_i I_\gamma - \mu_a M_a - \mu_m M_a I_2 - \mu_g M_a I_\alpha - \frac{\alpha_{12} M_a}{1 + \alpha_k B I_{10}}.
\end{aligned} \tag{3.3.19}$$

Thus, we have:

$$\mathcal{F} = \begin{pmatrix} \alpha_e B + \beta_i M_i + \mu_g N M_a I_\gamma \\ \alpha_r M_r B \\ 0 \end{pmatrix} \quad \text{and} \quad \mathcal{V} = \begin{pmatrix} \mu_B B \\ \left(\alpha_i I_\gamma + \mu_i - \alpha_{17} \pi_t T_0\right) M_i \\ \left(\mu_a + \mu_m I_2 + \mu_g I_\alpha + \frac{\alpha_{12}}{1 + \alpha_k B I_{10}}\right) M_a - \alpha_i M_i I_\gamma \end{pmatrix}$$

Therefore, we the linearisation of $\mathcal{F}$ and $\mathcal{V}$ at the MTB infection free equilibrium are given by:

$$F = \begin{pmatrix} \frac{\partial \mathcal{F}_1(E_0)}{\partial B} & \frac{\partial \mathcal{F}_1(E_0)}{\partial M_i} & \frac{\partial \mathcal{F}_1(E_0)}{\partial M_a} \\ \frac{\partial \mathcal{F}_2(E_0)}{\partial B} & \frac{\partial \mathcal{F}_2(E_0)}{\partial M_i} & \frac{\partial \mathcal{F}_2(E_0)}{\partial M_a} \\ \frac{\partial \mathcal{F}_3(E_0)}{\partial B} & \frac{\partial \mathcal{F}_3(E_0)}{\partial M_i} & \frac{\partial \mathcal{F}_3(E_0)}{\partial M_a} \end{pmatrix} = \begin{pmatrix} \alpha_e & \beta_i & 0 \\ \frac{\alpha_r \lambda_r}{\mu_r} & 0 & 0 \\ 0 & 0 & 0 \end{pmatrix}$$

and

$$V = \begin{pmatrix} \frac{\partial \mathcal{V}_1(E_0)}{\partial B} & \frac{\partial \mathcal{V}_1(E_0)}{\partial M_i} & \frac{\partial \mathcal{V}_1(E_0)}{\partial M_a} \\ \frac{\partial \mathcal{V}_2(E_0)}{\partial B} & \frac{\partial \mathcal{V}_2(E_0)}{\partial M_i} & \frac{\partial \mathcal{V}_2(E_0)}{\partial M_a} \\ \frac{\partial \mathcal{V}_3(E_0)}{\partial B} & \frac{\partial \mathcal{V}_3(E_0)}{\partial M_i} & \frac{\partial \mathcal{V}_3(E_0)}{\partial M_a} \end{pmatrix} = \begin{pmatrix} \mu_B & 0 & 0 \\ 0 & \frac{\mu_0\mu_i - \alpha_{17}\pi_t\lambda_0}{\mu_0} & 0 \\ 0 & 0 & \mu_a + \alpha_{12} \end{pmatrix}$$

We compute the inverse of V, denoted by V^{-1}, and given by:

$$V^{-1} = \begin{pmatrix} \frac{1}{\mu_B} & 0 & 0 \\ 0 & \frac{\mu_0}{\mu_0\mu_i - \alpha_{17}\pi_t\lambda_0} & 0 \\ 0 & 0 & \frac{1}{\mu_a + \alpha_{12}} \end{pmatrix}$$

Therefore, we obtain the next generation matrix $\mathcal{K}$, as follows:

$$\mathcal{K} = FV^{-1} = \begin{pmatrix} \frac{\alpha_e}{\mu_B} & \frac{\mu_0\beta_i}{\mu_i\mu_0 - \alpha_{17}\pi_t\lambda_0} & 0 \\ \frac{\alpha_r\lambda_r}{\mu_B\mu_r} & 0 & 0 \\ 0 & 0 & 0 \end{pmatrix}$$

The characteristic polynomial for the above matrix, $\mathcal{K}$ is given by:

$$\chi^2 - \frac{\alpha_e}{\mu_B}\chi - \frac{\mu_0\beta_i\alpha_r\lambda_r}{\mu_B\mu_r\left(\mu_0\mu_i - \alpha_{17}\lambda_0\pi_t\right)} = 0 \tag{3.3.20}$$

For simplicity, we condense the equation (3.3.20) such that:

$$\chi^2 - \chi\omega - \sigma = 0 \tag{3.3.21}$$

Thus, it follows that the roots for the above equation (3.3.21) are as follows:

$$\begin{aligned}\chi &= \frac{\omega \pm \sqrt{\omega^2 + 4\sigma}}{2}. \\ &= \frac{1}{2}\left(\omega + \sqrt{\omega^2 + 4\sigma}\right).\end{aligned}$$

Where

$\omega = \dfrac{\alpha_e}{\mu_B}$ represent the growth factor of *MTB*.

$$\sigma = \left(\frac{\beta_i}{\mu_B}\right)\left(\frac{\alpha_r\lambda_r}{\mu_r}\right)\left(\frac{\mu_0}{(\mu_0\mu_i - \alpha_{17}\lambda_0\pi_t)}\right) \tag{3.3.22}$$

The expression in equation (3.3.22) can be elucidated as follows:

$\left(\dfrac{\beta_i}{\mu_B}\right)$ represent the growth rate of *MTB* due to infected macrophages.

$\left(\dfrac{\alpha_r\lambda_r}{\mu_r}\right)$ represent the growth factor of rested macrophages after *MTB* infection.

$\dfrac{\mu_0}{(\mu_0\mu_i - \alpha_{17}\lambda_0\pi_t)}$ represent T cell growth factor after being primed by infected macrophages.

Since $\mathfrak{R}_o$ is the largest eigenvalue of the matrix, $\mathcal{K}$ or the spectral radius of the above matrix, $\mathcal{K}$.
Thus, the basic reproduction number is given by:

$$\mathfrak{R}_o = \frac{\omega + \sqrt{\omega^2 + 4\sigma}}{2}$$

The above expression (3.3.22) suggests that our $\mathfrak{R}_o$ depends greatly on the growth factors of M_r and T_0, respectively. In addition, the priming rate with the delay plays an important role in determining the outcome of the *MTB* infection. This supports the fact that for strong cellular immunity, priming rate with low time delay, T cell activation and macrophage recruitment are the keystone in facilitating and maintaining of the immune system.
In the next section 3.3.7.1 and section 3.3.7.2, we use the threshold of the reproductive number, $\mathfrak{R}_o < 1$. To analyse the stability of the system (3.2.14).

3.3.7 Stability of the infection-free equilibrium

3.3.7.1 Local stability of the infection-free equilibrium

To analyse local stability of the system (3.2.14). We show that if the eigenvalues of the Jacobian matrix have negative real parts. Therefore, the *MTB* infection free equilibrium, E_0, is locally asymptotically stable, i.e, $Re(\lambda_k) < 0$ and $\mathfrak{R}_o < 1$ [93].

Where

$$\{\lambda_k \in \mathbb{C} | k = 1, \ldots, 13\}$$

.

Consider the *MTB* infection free equilibrium Jacobian Matrix

$$J(E_0) = \begin{pmatrix}
-\mu_r & 0 & 0 & 0 & 0 & 0 & 0 & 0 & 0 & 0 & 0 & \frac{-\alpha_r\lambda_r}{\mu_r} & 0 \\
0 & \alpha_{17}\pi_t\frac{\lambda_0}{\mu_0} - \mu_i & 0 & 0 & 0 & 0 & 0 & 0 & 0 & 0 & 0 & \frac{\alpha_r\lambda_r}{\mu_r} & 0 \\
0 & 0 & -(\alpha_{12}+\mu_a) & 0 & 0 & 0 & 0 & 0 & 0 & 0 & 0 & 0 & 0 \\
0 & 0 & 0 & -d_\gamma & 0 & 0 & 0 & \alpha_{11} & 0 & 0 & 0 & 0 & 0 \\
0 & 0 & 0 & 0 & -d_2 & 0 & 0 & \alpha_{16} & 0 & 0 & 0 & 0 & 0 \\
0 & 0 & 0 & 0 & 0 & -d_\alpha & 0 & \alpha_{13} & 0 & 0 & 0 & 0 & 0 \\
0 & 0 & \alpha_{12} & 0 & 0 & 0 & -d_{12} & 0 & 0 & 0 & 0 & 0 & 0 \\
0 & C_1 & 0 & 0 & 0 & 0 & \frac{\alpha_{24}\lambda_0}{\mu_0} & \Theta & 0 & 0 & 0 & 0 & 0 \\
0 & 0 & 0 & 0 & 0 & 0 & 0 & 0 & -N & 0 & 0 & 0 & 0 \\
0 & 0 & 0 & 0 & 0 & 0 & 0 & 0 & 0 & -\mu_2 & 0 & \frac{\alpha_b\lambda_0}{\mu_0} & 0 \\
0 & C_4 & 0 & 0 & 0 & 0 & 0 & 0 & 0 & 0 & -d_{10} & C_5 & 0 \\
0 & \beta_i & 0 & 0 & 0 & 0 & 0 & 0 & 0 & 0 & 0 & \alpha_e - \mu_B & 0 \\
0 & C_6 & 0 & 0 & 0 & 0 & C_7 & 0 & 0 & 0 & 0 & C_8 & -\mu_0
\end{pmatrix}$$

Where

$$\Theta = -(\alpha_{13} + \pi_t + \alpha_1 + \alpha_{16}), C_1 = \alpha_{17}(1-\pi_t)\frac{\lambda_0}{\mu_0}, C_4 = \alpha_{17}\beta_{10}(1-\alpha_{treg})\frac{\lambda_0}{\mu_0},$$
$$C_5 = \frac{\alpha_{treg}\alpha_{10}\lambda_0}{\mu_0}, C_6 = -\frac{\alpha_{17}\lambda_0}{\mu_0} - C_5, C_7 = \frac{\alpha_{24}\lambda_0}{\mu_0}, C_8 = \frac{\alpha_b\lambda_0}{\mu_0} - C_5$$

To show local stability of the system at DFE, E_0, we proceed by applying the Geshgorin theorem [92] below.

Theorem 3.3.8. *Let $A = (c_{ij})_{1\leq i,j\leq n}$ be a matrix and $D_i = D(c_{ii}, r_i)$ be a disk in the complex plane centred at:*

$$r_i = \sum_{j=1, j\neq i}^{n} |c_{ii}|$$

and $\{\lambda_k, k = 1\ldots, n\}$ eigenvalues of A.
Then for all $i = 1, \ldots, n$, $\lambda_i \in \bigcup_{j=1}^{n} D_i$. Moreover, for an eigenvalue λ of A, $|\lambda - c_{ii}| \leq r_i$.

Since the Geshgorin theorem is applicable in the complex plane. We now employ it to our Jacobian matrix. The corollary 3.3.9 states and prove the Geshgorin theorem using the Jacobian matrix.

Corollary 3.3.9. *Let $A = (c_{ij})_{1\leq i,j\leq n}$ be a square diagonal matrix with real entries , such that the diagonal components of the square matrix A have the property $c_{ii} + r_i < 0$ then $c_{ii} < -r_i$.*

where

$$r_i = \sum_{j=1, j\neq i}^{n} |c_{ii}|$$

for all $i = 1, \ldots, n$. Therefore, all the eigenvalues λ_k, with $k = 1, \ldots, n$ have non-positive real parts.

We use the corollary 3.3.9 to examine the nature of the eigenvalues in the Jacobian matrix (3.3.7.1). Thus we obtain,

$$\mu_r > \frac{\alpha_r \lambda_r}{\mu_r}, \boxed{\alpha_{17}\pi_t \frac{\lambda_0}{\mu_0} - \mu_i > \frac{\alpha_r \lambda_r}{\mu_r}}, \alpha_{12} + \mu_a > 0$$

$$d_\gamma > \alpha_1, d_2 > \alpha_{16}, d_\alpha > \alpha_{13}, d_{12} > \alpha_{13}, C_6 > \frac{\alpha_b \lambda_0}{\mu_0} + \alpha_{treg}\alpha_{10}\frac{\lambda_0}{\mu_0},$$

$$\alpha_{17}\left(1-\pi_t\right)\frac{\lambda_0}{\mu_0} > \alpha_1 + \alpha_{16} + \alpha_{13} + \mu_1, \left(1-\pi_t\right)\beta_{10}\frac{\lambda_0}{\mu_0} > d_{10}$$

$$\boxed{\alpha_e - \mu_B > \beta_i} \tag{3.3.23}$$

Where

$$C_6 = -\frac{\alpha_{17}\lambda_0}{\mu_0} - \left(1-\alpha_{treg}\right)\beta_{10}\frac{\lambda_0}{\mu_0}.$$

To show that IFE is stable i.e., ($\Re_o < 1$). We consider the expressions which are boxed in (3.3.23), we combine them to obtain,

$$\alpha_{17}\pi_t\lambda_0\mu_r\alpha_e - \mu_i\mu_r\alpha_e\mu_0 + \alpha_{17}\pi_t\lambda_0\mu_r\mu_B - \mu_i\mu_r\mu_B\mu_0 > \alpha_r\lambda_r\mu_0\beta_i.$$

This implies that

$$\left(\frac{\alpha_r\lambda_r\mu_0\beta_i}{\mu_i\mu_r\mu_B\mu_0-\alpha_{17}\pi_t\lambda_0\mu_r\mu_B}\right)+\frac{\alpha_e\left(\mu_i\mu_0-\alpha_{17}\pi_t\lambda_0\right)}{\mu_B\left(\mu_i\mu_0-\alpha_{17}\pi_t\lambda_0\right)}.$$

Let

$$\frac{\alpha_r\lambda_r\mu_0\beta_i}{\mu_i\mu_r\mu_B\mu_0-\alpha_{17}\pi_t\lambda_0\mu_r\mu_B}+\frac{\alpha_e}{\mu_B}<1.$$

Indeed, we know that for local stability of E_0, $\mathfrak{R}_o<1$, such that

$$\mathfrak{R}_o=\frac{\omega+\sqrt{\omega^2+4\sigma}}{2}<1.$$

This implies that

$$\mathfrak{R}_o=\left(\sqrt{\omega^2+4\sigma}\right)^2<(2-\omega)^2. \tag{3.3.24}$$

Simplifying the above equation (3.3.24) we obtain

$$\mathfrak{R}_o=\omega+\sigma<1.$$

Thus, we see that

$$\mathfrak{R}_o=\frac{\alpha_r\lambda_r\mu_0\beta_i}{\mu_i\mu_r\mu_B\mu_0-\alpha_{17}\pi_t\lambda_0\mu_r\mu_B}+\frac{\alpha_e}{\mu_B}<1.$$

Since

$$\omega=\frac{\alpha_e}{\mu_B}\quad\text{and}\quad\sigma=\frac{\alpha_r\lambda_r\mu_0\beta_i}{\mu_i\mu_r\mu_B\mu_0-\alpha_{17}\pi_t\lambda_0\mu_r\mu_B}.$$

Therefore, we conclude that the *MTB* infection free equilibrium E_0, is locally asymptotically stable.

3.3.7.2 Global stability of the infection-free equilibrium

In order to establish the global asymptotic stability, we use the Castillo-Chavez et al, [95] approach by rewritting the system of differential equations (3.2.14) as follows:

$$\frac{dZ}{dt} = F(Z, Y)$$

$$\frac{dY}{dt} = G(Z, Y) \quad \text{with} \quad G(Z, 0) = 0,$$

where $Y \in \mathbb{R}^m$ and $Z \in \mathbb{R}^n$ denote compartments describing the number of infected and uninfected cells, respectively. Let E_0 be the *MTB* infection free equilibrium, the two following conditions must be satisfied:

$$(I) \quad \frac{dZ}{dt} = F(Z, 0), \quad E_0 \quad \text{is globally asymptotically stable.}$$

$$(II) \quad \hat{G}(Z, Y) = AY - G(Z, Y), \quad \hat{G}(Z, Y) \geq 0 \quad \text{for all} \quad (Z, Y) \in \Omega.$$

Where $A = D_z G(E_0, 0)$ is a Jacobian matrix of $\hat{G}(Z, Y)$ evaluated at the infection free equilibrium, which is a metzler matrix (with non-negative-off diagonal components).

Lemma 3.3.10. *For the system* (3.2.14)*, global asymptotic stability cannot be guaranteed.*

Apply the Castillo-Chavez approach to the system (3.2.14), we get:

$$\frac{dZ}{dt} = F(Z,0) = \begin{bmatrix} \lambda_r - \mu_r M_r \\ \frac{\alpha_1 T_1}{1+\alpha_{25} I_{10}} - d_\gamma I_\gamma \\ \frac{\alpha_{16} T_1}{1+\alpha_{25} I_{10}} - d_2 I_2 \\ \alpha_{15} T_2 I_{10} - d_4 I_4 \\ \frac{\alpha_{13} T_1}{1+\alpha_{25} I_{10}+\alpha_4 I_4} - d_\alpha I_\alpha \\ -d_{10} I_{10} \\ -d_{12} I_{12} \\ \lambda_0 - \frac{\alpha_{24} T_0 I_{12}}{1+\alpha_4 I_4} - \mu_0 T_0 \\ -\frac{\alpha_1 T_1}{1+\alpha_{25} I_{10}} - \frac{\alpha_{13} T_1}{1+\alpha_{25} I_{10}+\alpha_4 I_4} - \frac{\alpha_{16} T_1}{1+\alpha_{25} I_{10}} + \frac{\alpha_{24} T_0 I_{12}}{1+\alpha_4 I_4} - \mu_1 T_1 \\ -\alpha_{15} T_2 I_{10} - \mu_2 T_2 \end{bmatrix}$$

$$\frac{dY}{dt} = \begin{bmatrix} \alpha_r M_r B - \alpha_i M_i I_\gamma + \alpha_{17} \pi_t M_i T_0 - \mu_i M_i \\ \alpha_i M_i I_\gamma - \mu_a M_a - \mu_m M_a I_2 - \mu_g M_a I_\alpha - \frac{\alpha_{12} M_a}{1+\alpha_k B I_{10}} \\ \alpha_e B + \beta_i M_i + \mu_g N M_a I_\alpha - \mu_B B \end{bmatrix}$$

where

$$Z = \left[M_r, I_\gamma, I_2, I_4, I_\alpha, I_{10}, I_{12}, T_0, T_1, T_2 \right]^T \quad \text{and} \quad Y = \left[M_i, M_a, B \right]^T$$

The Jacobian matrix A is given by:

$$A = \begin{bmatrix} \alpha_{17}\pi_t \frac{\lambda_0}{\mu_0} - \mu_i & 0 & \alpha_r \frac{\lambda_r}{\mu_r} \\ 0 & -(\mu_a + \alpha_{12}) & 0 \\ \beta_i & 0 & \alpha_e - \mu_B \end{bmatrix}$$

such that

$$AY = \begin{bmatrix} \alpha_{17}\pi_t \frac{\lambda_0}{\mu_0} - \mu_i & 0 & \alpha_r \frac{\lambda_r}{\mu_r} \\ 0 & -(\mu_a + \alpha_{12}) & 0 \\ \beta_i & 0 & \alpha_e - \mu_B \end{bmatrix} \begin{bmatrix} M_i \\ M_a \\ B \end{bmatrix} = \begin{bmatrix} \left(\alpha_{17}\pi_t \frac{\lambda_0}{\mu_0} - \mu_i\right) M_i + \alpha_r \frac{\lambda_r}{\mu_r} B \\ -(\mu_a + \alpha_{12}) M_a \\ \beta_i M_i + (\alpha_e - \mu_B) B \end{bmatrix}$$

Thus,

$$\hat{G}(Z,Y) = AY - G(Z,Y)$$

$$= \begin{bmatrix} \left(\alpha_{17}\pi_t \frac{\lambda_0}{\mu_0}\right) M_i - \alpha_r M_r B + \alpha_i M_i I_\gamma - \alpha_{17}\pi_t M_i T_0 + \alpha_r \frac{\lambda_r}{\mu_r} B \\ -\alpha_i M_i I_\gamma + \mu_m M_a I_2 - \alpha_{12} M_a + \mu_g M_a I_\alpha + \frac{\alpha_{12} M_a}{1+\alpha_k B I_{10}} \\ \mu_g N M_a I_\alpha \end{bmatrix} = \begin{bmatrix} \hat{G}_1(Z,Y) \\ \hat{G}_2(Z,Y) \\ \hat{G}_3(Z,Y) \end{bmatrix}$$

we have:

$$\hat{G}_1(Z,Y) = \alpha_{17}\pi_t M_i \left(\frac{\lambda_0}{\mu_0} - T_0\right) + \alpha_r B \left(\frac{\lambda_r}{\mu_r} - M_r\right) + \alpha_i M_i I_\gamma$$

It follows that $\hat{G}_1(Z,Y) \geq 0$, since $\frac{\lambda_r}{\mu_r} - M_r \geq 0$ and $\frac{\lambda_0}{\mu_0} - T_0 \geq 0$, as there is no infection at the *MTB* infection free equilibrium.

Furthermore, $\hat{G}_3(Z,Y) = \mu_g N M_a I_\alpha \geq 0$, since all parameters are positive and state variables are non-negative.

Finally

$$\hat{G}_2(Z,Y) = -\alpha_i M_i I_\gamma + \mu_m M_a I_2 - \alpha_{12} M_a + \mu_g M_a I_\alpha + \frac{\alpha_{12} M_a}{1+\alpha_k B I_{10}}.$$

$$= -\alpha_{12} M_a - \mu_a M_a - \left(\alpha_i M_i I_\gamma - \mu_m M_a I_2 - \mu_a M_a - \mu_g M_a I_\alpha - \frac{\alpha_{12} M_a}{1+\alpha_k B I_{10}} \right).$$

In case of *MTB* infection, M_a is expected to increase and when there is no infection $M_a = 0$, which suggests that

$$\frac{dM_a}{dt} \geq 0 \quad \text{or} \quad \alpha_i M_i I_\gamma - \mu_m M_a I_2 - \mu_a M_a - \mu_g M_a I_\alpha - \frac{\alpha_{12} M_a}{1+\alpha_k B I_{10}},$$

implying

$$\hat{G}_2(Z,Y) \leq -\left(\alpha_{12} + \mu_a\right) M_a.$$

This implies that $\hat{G}_2(Z,Y) \leq 0$ as all parameters and state variables are positive. Thus, since $\hat{G}_2(Z,Y) \leq 0$, i.e., the condition (II) is not fulfilled, the global asymptotic stability cannot be guaranteed.

In this chapter, we presented the Tuberculosis micro-environment scheme and described the cell equations for the system (3.2.14). In addition, we performed model analysis, which includes, positivity of solutions, feasibility of solutions and stability analysis of the *MTB* infection free equilibrium. In the next chapter, we present and describe the methods used to fit the model to experimental data. We use the reproductive number, $\mathfrak{R}_o$, to analyse the behaviour of the cell populations.

Chapter 4

Results and Discussion

In this chapter, we numerically solve our system (3.2.14) and track cell behaviours over time. Intuitively, we fit our model to experimental data to obtain parameter values that best describe the cell behaviours during *MTB* infection. Additionally, we project the outcome of *MTB* infection over time. The procedure for model fitting is described in section 4.1.1 and section 4.1.2, respectively.

4.1 Estimation of parameters

We use non-linear least square (NLS) and Markov Chain Monte Carlo (MCMC) methods, to estimate parameter values. For the MCMC, The Bayesian inference, with the likelihood function and prior probability is employed to calculate the posterior probability. The results from MCMC can be represented graphically.

4.1.1 Non-linear Least Square (NLS) Method

We first let $t \in \mathbb{R}$ represent time, and $y \in \mathbb{R}^{13}$ be a vector of state variables. Let $\theta \in \mathbb{R}$ be a vector with model parameters and f be a function such that $f(t, y, \theta)$. Then our system (3.2.14) can be written as,

$$\begin{cases} \frac{d}{dt}y(t,\theta) & = f(t,y,\theta), \\ y(0,\theta) & = y_0, \end{cases} \tag{4.1.1}$$

where $y(0,\theta) = y_0$ represent the initial conditions.
The aim of the NLS is to minimise the the sum of squares of errors (SSE) from the actual data values, $y(t_i)$ and the model predicted values $\hat{y}(t_i)$ which depends on the list of

parameters θ. For any n data points (t_i, y_i), where $i = \{1, \ldots, n\}$. The objective is to minimize the error using the function below

$$M(\theta) = \sum_{i=1}^{n} [\hat{y}(t_i) - y(t_i)]^2. \tag{4.1.2}$$

Suppose that $m \geq n$ and $\mathbb{R}^n \mapsto \mathbb{R}^m$. For $i = \{1, \ldots, m\}$, where m is the estimated parameters. We want to compute the parameter values (θ) fitting our model. Therefore,

$$\min_{\theta} M(\theta) \quad \text{such that} \quad \theta_{min} \leq \theta_i \leq \theta_{max}. \tag{4.1.3}$$

The above (4.1.3) optimization problem is solved under R, using the desolve package. Likewise, the optim package is used to fit our model to the actual data in [84].

4.1.2 Markov Chain Monte Carlo (MCMC) Method

Definition 4.1.1. *Prior probability - is the probability of observing parameters before an event or data samples.*

Definition 4.1.2. *Posterior probability - is the probability of observing parameters with the availability of data samples.*

We now explore the Bayesian-based MCMC method, to inspect the fitted values obtained from the NLS method. We obtain the probability distribution of our model parameters based on the actual data. The posterior distribution is given by $\mathbb{P}(\theta|y)$. To evaluate the posterior distribution, we consider the product of the likelihood $\mathbb{P}(y|\theta)$ and prior distribution $\mathbb{P}(\theta)$, respectively.

Given $\hat{y}(t_i)$ of the system (3.2.14), for the actual data y, with the model parameter θ. We have that,

$$y(\theta) = \hat{y}(t_i) + \varepsilon, \tag{4.1.4}$$

where ε is the error term, which is the normally distributed Gaussian noise, with mean $\mu = 0$ and variance δ, denoted by $\varepsilon \sim \mathcal{N}(0, \delta)$. From the Bayes' theorem we have,

$$\mathbb{P}(\theta|y, \delta) = \frac{\mathbb{P}(y|\theta, \delta)\mathbb{P}(\theta, \delta)}{\mathbb{P}(y, \delta)}, \tag{4.1.5}$$

where $\mathbb{P}(y,\delta) \neq 0$ denotes the probability of the actual data. However, since $\mathbb{P}(y,\delta)$ is a constant used for normalisation. It follows that,

$$\mathbb{P}(\theta|y,\delta) \propto \mathbb{P}(y|\theta,\delta)\mathbb{P}(\theta,\delta). \tag{4.1.6}$$

We apply the natural logarithm to scale the posterior probability $\mathbb{P}(\theta|y,\delta)$, between 0 and 1, respectively. We obtain,

$$\ln(\mathbb{P}(\theta|y,\delta)) = \ln(\mathbb{P}(y|\theta,\delta)) + \ln(\mathbb{P}(\theta,\delta)), \tag{4.1.7}$$

Since the likelihood $\mathbb{P}(y|\theta,\delta)$ is generally represented by $L(y,\theta,\delta)$. Therefore,

$$\ln(\mathbb{P}(\theta|y,\delta)) = \ln(L(y,\theta,\delta)) + \ln(\mathbb{P}(\theta,\delta)), \tag{4.1.8}$$

where

$$L(y,\theta,\delta) = \prod_{i=1}^{n} \frac{1}{\delta y_i \sqrt{2\pi}} \exp\left(-\frac{1}{2}\left(\frac{\ln(y_i) - \hat{y}_i}{\delta}\right)^2\right). \tag{4.1.9}$$

We assume the actual data y are independently and identically distributed, denoted by $y \overset{iid}{\sim} \mathcal{N}(0,\delta)$. And also, the model prior has equal probabilities. After substituting (4.1.9) in equation (4.1.8), we obtain

$$\ln(L(y,\theta,\delta)) = -\sum_{i=1}^{n}\left(\ln(\delta y_i\sqrt{2\pi}) + \frac{1}{2}\left(\frac{\ln(y_i) - \hat{y}_i}{\delta}\right)^2\right)$$

$$\Rightarrow \ln(L(y,\theta,\delta)) = -\sum_{i=1}^{n}\left(\ln(\delta) + \ln(y_i) + \frac{1}{2}\left[\ln(2\pi) + \frac{1}{\delta^2}\left(\ln(y_i) - \hat{y}_i\right)^2\right]\right).$$

To fit our model to experimental data on the dynamics of *MTB* infection. We use R software to compute the Bayesian framework. The experimental data can be accessed in [84].

4.2 Estimated values and fitted plots

In this section, we perform curve fitting to the observed data, using the NLS and MCMC methods, respectively. The results of our best model (3.2.14) fit is represented by Figure 4.2. Of these, we use the parameter values estimated by the NLS method, presented in Table 4.2. We adopt 18 parameter values from experimental studies.

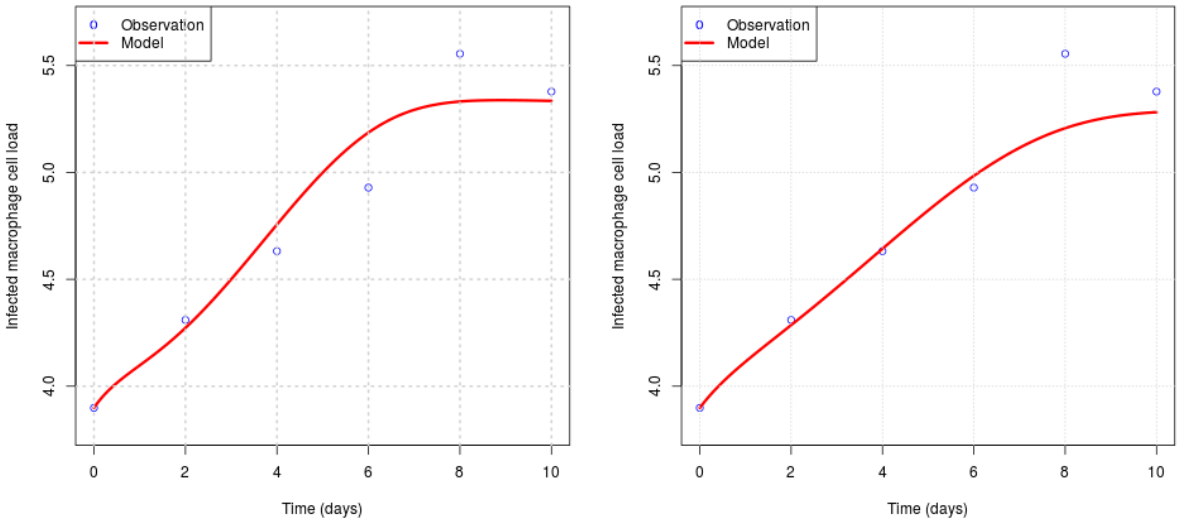

(a) NLS method (b) MCMC method

Figure 4.1: The plot showing curve fitting of infected macrophages of model (3.2.14) to experimental data of *MTB* infection.

Parameter	Description	NLS value	MCMC value	Units	Source
λ_0	source of T_0	0.99	0.99	cells/ml/day	Assumed
λ_r	source of resident macrophages from monocytes	0.99	0.99	cells/ml/day	Assumed
α_1	production rate of the I_γ by T_1	0.18193615	0.601614030	1/day	Estimated
α_4	inhibition rate of the I_α and M_a proliferation by I_4	$9.948914e-01$	0.585353464	1/day	Estimated
α_{10}	the ability of the B to subvert I_{10} capacity	$2.941191e-04$	0.452665121	pg/ cell day	Estimated
α_{12}	production rate of I_{12} by M_a	$9.941308e-01$	0.620366177	pg/ cell day	Estimated
α_{13}	production rate of I_α by T_1	0.31	0.31	pg/cell day	[14]
α_{15}	production rate of I_4 by T_2	2.18×10^{-2}	2.18×10^{-2}	pg/cell day	[14]
α_{16}	production rate of I_2 by T_1	0.12	0.12	pg/cell day	[14]
α_{17}	priming rate of T_0 by M_i	$1.000000e-07$	0.783815492	ml/cell/day	[14]
α_{25}	inhibition rate of I_γ response by I_{10}	$9.950000e-01$	0.351887193	1/day	Estimated
α_b	priming rate of T_2 response by B	$1.798849e-05$	0.576115658	ml/cell/day	Estimated
α_e	growth rate of B	0.30	0.30	1/day	[14]
α_i	macrophage activation rate for M_i due to I_γ	$1.000000e-07$	0.000000100	ml/cell/day	Estimated
α_k	inhibition rate of I_{12} production by B using I_{10}	$9.765557e-01$	0.619729307	1/day	Estimated
α_r	macrophage infection rate of M_i due to B	$4.849652e-03$	0.004395126	ml/cell/day	Estimated
β_i	the capacity of M_i to reduce the bacterial load of B	0.17×10^{-2}	0.17×10^{-2}	cell^{-1}	[14]
β_{10}	the capacity of T_0 to differentiate	0.0005	0.0005	ml/cell/day	Estimated
α_{treg}	the capacity of the I_{10} to promote T_2 response	$9.751985e-01$	0.760965613	pg/ cell day	Estimated
$1-\alpha_{treg}$	the capacity of the I_{10} to inhibit T_1 response	0.0248015	0.314356054	pg/ cell day	Estimated
μ_0	per capita death rate of T_0 due to apoptosis	0.3333/500000	0.3333/500000	1/day	[14]
μ_1	per capita death rate of T_1 due to apoptosis	0.3333	0.3333	1/day	[14]
μ_2	per capita death rate of T_2 due to apoptosis	0.3333	0.3333	1/day	[14]
μ_a	per capita death rate of M_a due to apoptosis	0.011	0.011	1/day	[14]
μ_g	per capita death rate of M_a due to bursting	$2.716486e-03$	0.676791106	1/day	Estimated
μ_m	per capita death rate of M_a due to I_2	$1.844496e-02$	0.571452346	1/day	Estimated
μ_i	per capita death rate of M_i due to apoptosis	0.011	0.011	1/day	[14]
μ_r	per capita death rate of M_r due to apoptosis	0.011	0.011	1/day	[14]
μ_B	per capita death rate of B	$9.936898e-01$	0.370371992	1/day	Estimated
d_γ	degradation rate of I_γ	2.16×10^{-2}	2.16×10^{-2}	1/ day	[14]
d_2	degradation rate of I_2	$9.765884e-01$	0.763905182	1/ day	Estimated
d_4	degradation rate of I_4	2.77×10^{-2}	2.77×10^{-2}	1/ day	[14]
d_α	degradation rate of T_α	$4.143186e-01$	0.396063829	1/day	Estimated
d_{10}	degradation rate of I_{10}	3.6968×10^{-2}	3.6968×10^{-2}	1/ day	[14]
d_{12}	degradation rate of I_{12}	1.188×10^{-2}	1.188×10^{-2}	1/ day	[14]
π_t	time delay of T_0 priming by M_i	$1e-10$	$1e-10$	ml/cell/day	[14]
N	number of released bacteria by M_a , as a result of multiplicity of infection (MOI)	100	100		[14]

4.3 Numerical simulations

In this section 4.3, we perform numerical simulations for the system (3.2.14). The parameter values used are obtained in Table 4.2, from the NLS method. In addition, we investigated the switching time from M_i to M_a, and behaviours of cytokines I_γ, I_{12}, which are responsible for macrophage activation and proliferation. We notice that when

$\mathfrak{R}_o > 1$ switching time from M_i to M_a occurs faster, which is approximately after 8 days. However, when $\mathfrak{R}_o < 1$, the macrophages (M_i to M_a) switch approximately after 9 days. This dynamics are presented in Figure 4.2a and Figure 4.2b. In addition, from Figure 4.4a and Figure 4.4b, we observe that I_{12} increased whenever $\mathfrak{R}_o < 1$ and $\mathfrak{R}_o > 1$. This suggests that macrophages (M_a) proliferate efficiently. However, for $\mathfrak{R}_o < 1$, the observed increase of I_γ in Figure 4.3a is sufficient to maintain the macrophage activation. The results in Figure 4.3b shows the increase of I_γ, which is compromised by anti-microbial activities or other factors. This suggest the need for I_γ to maintain macrophage activation.

To explore the effect of $\mathfrak{R}_o$ on T cells response and the switching of the protective immunity, from pro-inflammatory to anti-inflammatory immune response. We consider T_1 and T_2, represented by Figure 4.5a and Figure 4.5b. We can see that $\mathfrak{R}_o > 1$ is associated with deficiency of T_1. This might be due to *MTB* promoting T_2 response to impede anti-microbial perturbations. The cytokines I_α and I_4 are more likely candidates for this switch (T_1 to T_2).

I_α dynamics are very interesting. The results in Figure 4.9b and Figure 4.6b shows that in both cases of the reproductive number, i.e., $\mathfrak{R}_o < 1$ and $\mathfrak{R}_o > 1$. The I_α is highly expressed and this is associated with *MTB* dissemination. This supports the findings that low and high I_α leads to bacterial persistence [23, 66].

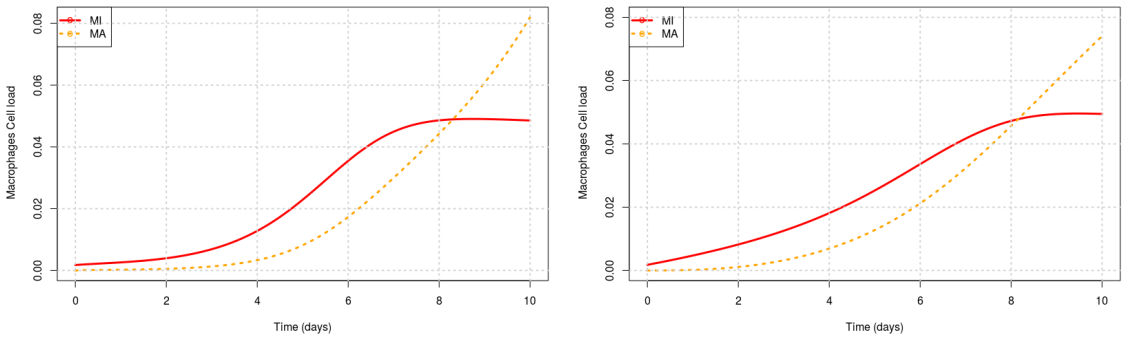

(a) The effect of $\mathfrak{R}_o < 1$

(b) The effect of $\mathfrak{R}_o > 1$

Figure 4.2: The plot showing the effect of stability on the switching time from M_i to M_a.

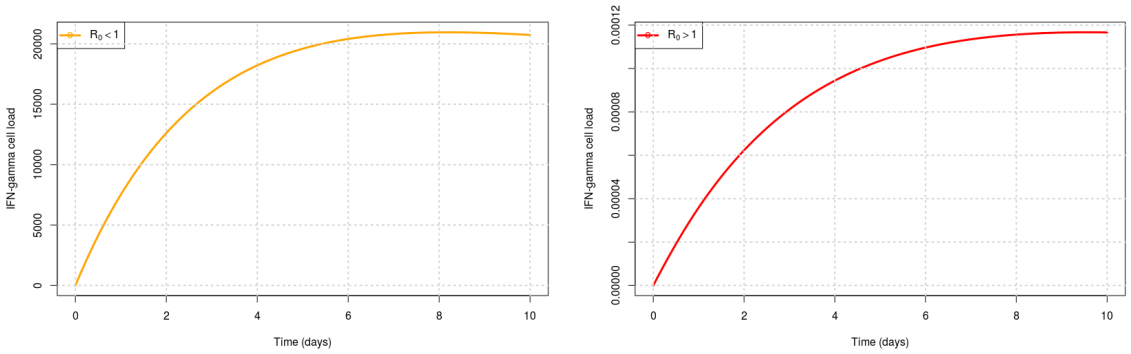

(a) The concentration of the I_γ when $\mathfrak{R}_o < 1$. (b) The concentration of the I_γ when $\mathfrak{R}_o > 1$.

Figure 4.3: The plot showing the effect of stability on the concentration of the IFN-γ.

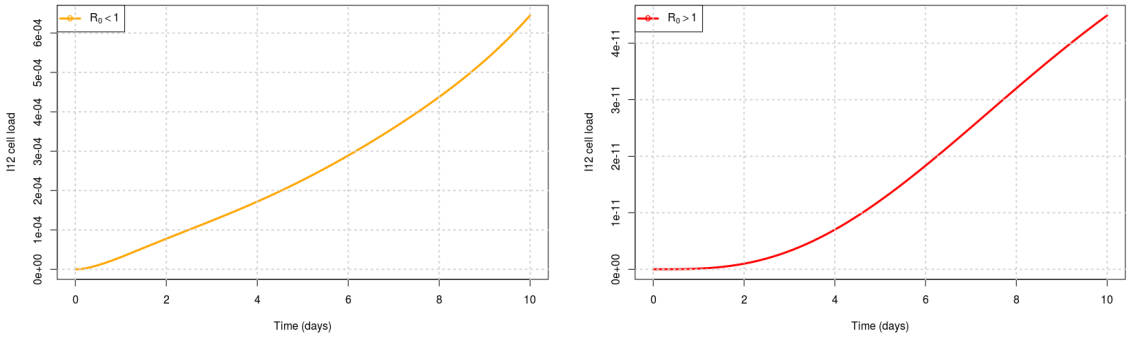

(a) The concentration of the I_{12} when $\mathfrak{R}_o < 1$. (b) The concentration of the I_{12} when $\mathfrak{R}_o > 1$.

Figure 4.4: The plot showing the effect of stability on the concentration of the I_{12}.

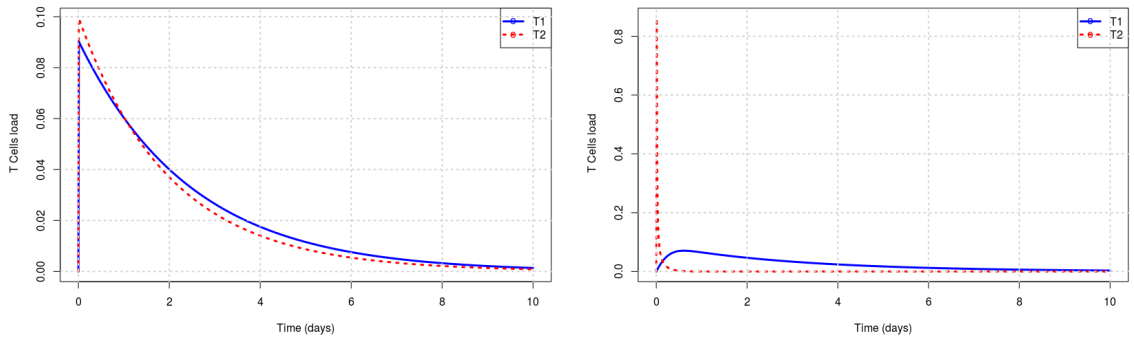

(a) The effect of $\mathfrak{R}_o < 1$ on T_1 and T_2 response. (b) The effect of $\mathfrak{R}_o > 1$ on T_1 and T_2 response.

Figure 4.5: The plot indicating the effect of stability on the concentrations of the T_1 and T_2.

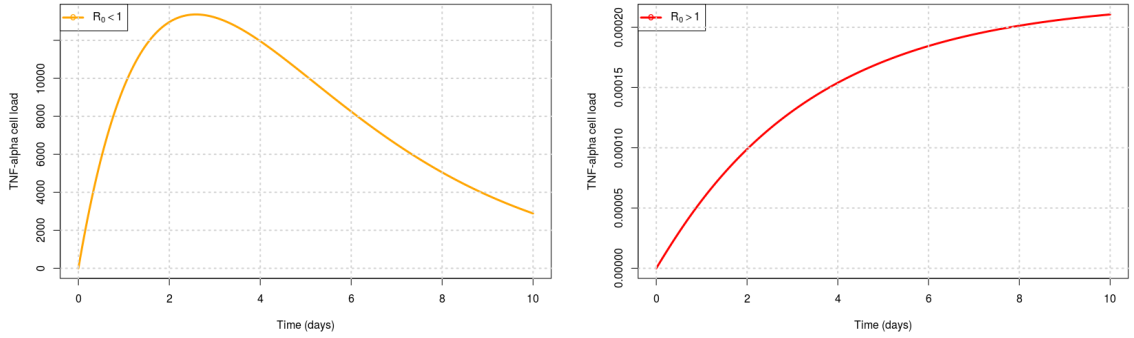

(a) The concentration of the I_α when $\mathfrak{R}_o < 1$. (b) The concentration of the I_α when $\mathfrak{R}_o > 1$.

Figure 4.6: The plot showing the effect of stability on the concentration of the TNF-α.

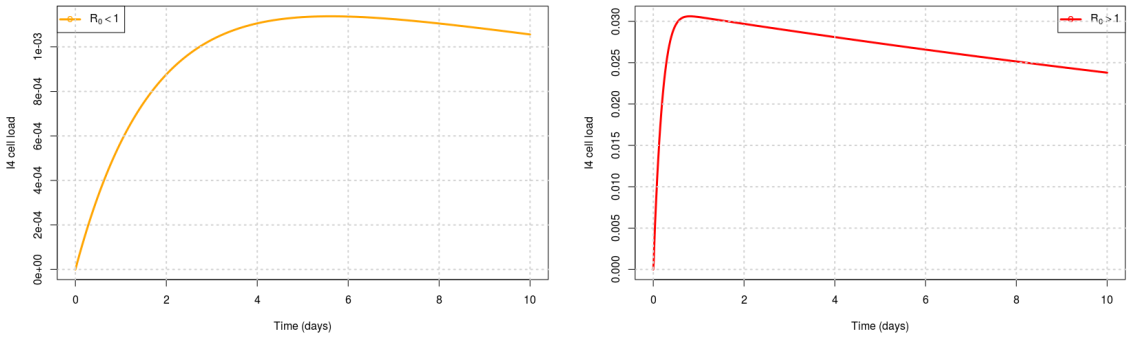

(a) The concentration of the I_4 when $\mathfrak{R}_o < 1$. (b) The concentration of the I_4 when $\mathfrak{R}_o > 1$.

Figure 4.7: The plot showing the effect of stability on the concentration of the I_4.

In the next section 4.4, we discuss the parameter values altering the dynamics of the system (3.2.14).

4.4 Sensitivity analysis

To observe the effect of the time delay π_t on the reproductive number. We project the *MTB* infection by performing simulations for 20 days. As anticipated, when $\mathfrak{R}_o < 1$, the *MTB* infection is contained by the immune system, as seen in Figure 4.9a, the *MTB* load is dropping. In addition, from the results in Figure 4.8a, we can see that the density of the infected macrophages drops because the *MTB* load is killed. This correlates with the results in Figure 4.10a of IL-2. However, when $\mathfrak{R}_o > 1$, the results in Figure 4.9b shows the exponential growth of the *MTB* infection. We also notice in Figure 4.8b that the density of infected macrophages is very high, it levels off with a density of 200000 cells/ml/day.

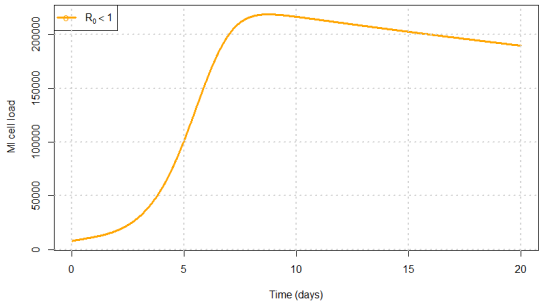

(a) The M_i cell load when $\mathfrak{R}_o < 1$.

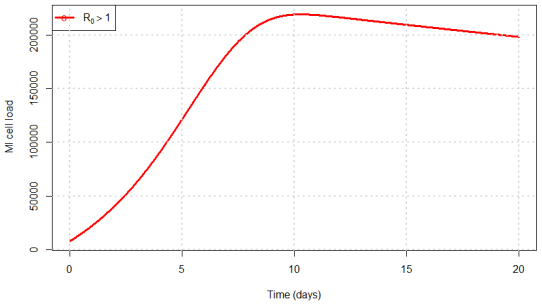

(b) The M_i cell load when $\mathfrak{R}_o > 1$.

Figure 4.8: The plot showing the effect of stability on the M_i cell load.

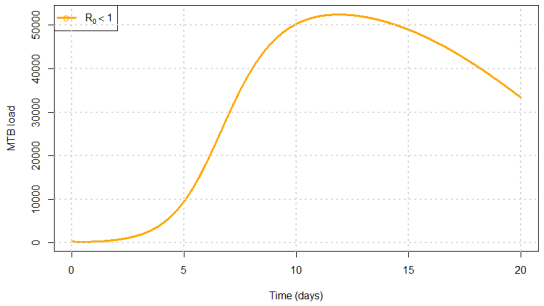

(a) The plot indicating *MTB* load

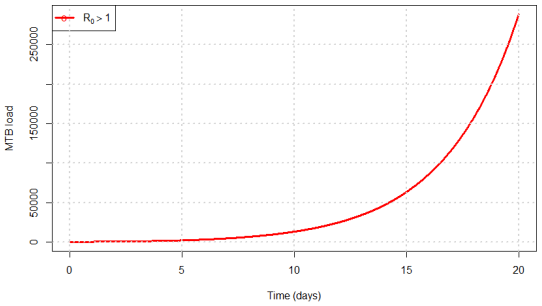

(b) The plot indicating *MTB* load

Figure 4.9: The plot showing the effect of stability on the *MTB* load.

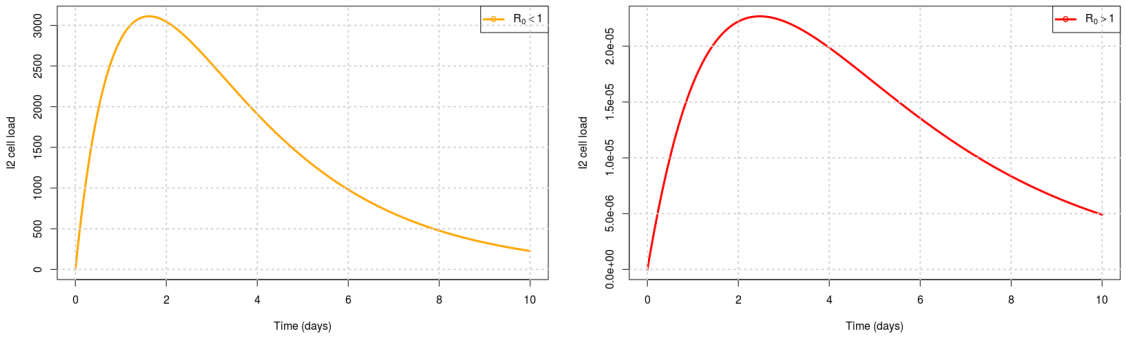

(a) The concentration of the I_2 when $\mathfrak{R}_o < 1$. (b) The I_2 concentration when $\mathfrak{R}_o > 1$.

Figure 4.10: The plot showing the effect of stability on the concentration of the I_2.

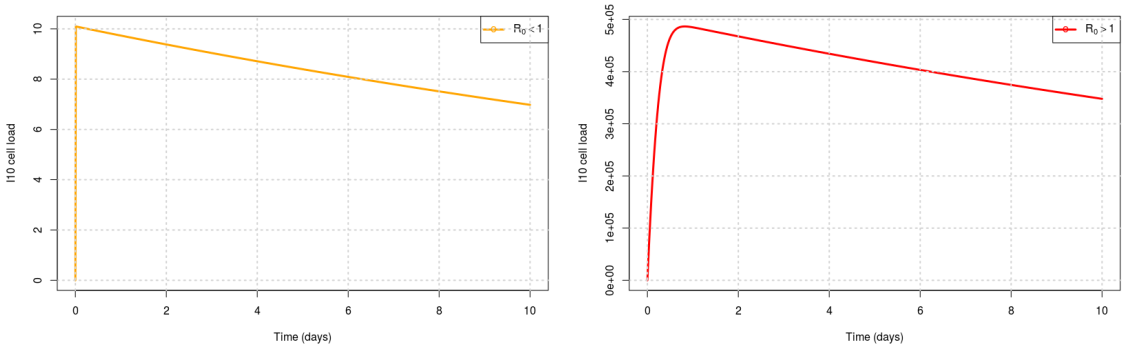

(a) The I_{10} concentration when $\mathfrak{R}_o < 1$. (b) The I_{10} concentration when $\mathfrak{R}_o > 1$.

Figure 4.11: The plot showing the effect of stability on the concentration of the I_{10}.

The results from the above Figure 4.10b shows that the infected cells killing by I_2 drops faster when the system (3.2.14) is unstable. This failure of cells killing by I_2 leads to the granuloma formation. As anticipated, the increase in I_{10} concentration is associated with unstable, $\mathfrak{R}_o > 1$, of the immune system, see Figure 4.11b. Although I_{10} prevent tissue damage and inflammation. The ability of I_{10} to promote *MTB* growth is supported by the results in Figure 4.11b. Furthermore, this support the findings that I_{10} is associated with high *MTB* load [58, 76].

The summary of the results of how the cells are expressed, are presented in the following Table 4.1.

Table 4.1: Summary of the results.

Variables	$\mathfrak{R}_o < 1$	$\mathfrak{R}_o > 1$	Range when $\mathfrak{R}_o < 1$	Range when $\mathfrak{R}_o > 1$	Units
M_r	decrease	decrease	$(0, 4e+05)$	$(0, 4e+05)$	cells/ml
M_i	increase	increase	$(0, 217682)$	$(0, 219530)$	cells/ml
M_a	decrease	decrease	$(0, 533)$	$(0, 0.0295)$	cells/ml
I_γ	increase	decrease	$(0, 20955)$	$(0, 0.0001166893)$	pg/ml
I_2	increase	decrease	$(0, 3111)$	$(0, 2.268018e-05)$	pg/ml
I_4	decrease	increase	$(0, 0.001137401)$	$(0, 0.03060683)$	pg/ml
I_α	decrease	increase	$(0, 13366)$	$(0, 0.0002106935)$	pg/ml
I_{10}	decrease	increase	$(0, 10)$	$(0, 486665)$	pg/ml
I_{12}	decrease	increase	$(0, 0.01148372)$	$(0, 4.491276e-11)$	pg/ml
T_0	increase	decrease	$(0, 5e+05)$	$(0, 5e+05)$	pg/ml
T_1	decrease	decrease	$(0, 498064)$	$(0, 85)$	pg/ml
T_2	increase	increase	$(0, 0.003471331)$	$(0, 0.0004382745)$	pg/ml
MTB	decrease	increase	$(0, 40396)$	$(0, 289049)$	pg/ml

From the above Table 4.1, the second and third rows represent how the change in stability affect the cells behaviour. The last three rows represent the biological range of the cells with respect to the stability. The remaining last row shows the units of the state variables in the system (3.2.14). We observe that the increase in the anti-inflammatory response is associated with *MTB* persistence.

In this chapter, we performed curve fitting to model (3.2.14), using the NLS and MCMC methods, respectively. In addition, we further explore the dynamics of the *MTB* infection by performing numerical simulations and sensitivity analysis. In section 4.4, we performed numerical simulations to track the behaviour of the system (3.2.14). We analysed the system (3.2.14) based on the reproductive number, $\mathfrak{R}_o$. We noticed that when $\mathfrak{R}_o < 1$, the system (3.2.14) is able to contain the *MTB* infection. However, when $\mathfrak{R}_o > 1$, the *MTB* persists resulting in over-expression of the anti-inflammatory immune response. In the next chapter, we use findings from our analysis to make concluding remarks.

Chapter 5

Conclusion

In this study, we developed a mathematical scheme aimed at elucidating the cellular dynamics of the human immune response to *MTB* infection. This scheme incorporated and described the key roles of the different cells compartments of macrophages, T cells and cytokines, respectively. For macrophages, we considered intracellular *MTB* within macrophages and tracked the process of phagocytosis. In addition, we included the time delay to account for the microbial perturbations by *MTB*, in defence to anti-microbial activities by macrophages. The extracellular bacteria is captured by including the dummy parameter N, for released bacterial load after failure of phagocytosis.

Furthermore, we inspected and analysed the dynamics of T cells response, both pro-inflammatory and anti-inflammatory. For pro-inflammatory, we examined the roles of four potent cytokines namely, IFN-γ, TNF-α, IL-2 and IL-12. The biology and roles of this cytokines are well addressed in Chapter 3. In addition, we looked at two regulatory cytokines IL-4 and IL-10, respectively. In fact, our focal point was to analyse how regulatory cytokines affect the stability of the protective immunity.

We employed the non-least square (NLS) and Markov Chain Monte Carlo (MCMC) methods to fit our system (3.2.14) to the observed data in [84], on mice infected with *MTB*. To analyse our results, we use the reproductive number thresholds $\mathfrak{R}_o < 1$ and $\mathfrak{R}_o > 1$ as our factor. The results from this fit showed progression of the *MTB* infection when the time delay is increased. In fact, from the numerical simulations and sensitivity analysis, when the time delay is increased the system (3.2.14) is unstable (i.e, $\mathfrak{R}_o > 1$). This suggest there are more infected macrophages, leading to high *MTB* load. To analyse this impediment, we looked at the switching time (M_i to M_a) and infected cell killing

by IL-2. In Figure 4.2b, we see that the switching time decrease when time delay is increased. This point out insight on the inefficiency of cell termination by IL-2. Indeed, the Figure 4.10b shows that the time delay negatively affects cytotoxicity of IL-2.

The cytokines IFN-γ, TNF-α, IL-2 can be considered to be amplified for TB vaccine design. Although the levels of IFN-γ collapsed when $\mathfrak{R}_o > 1$. This is due to the deficiency of the type 1 helper T cells. Thus, IFN-γ remains the potent cytokine for protective immunity against *MTB* infection. The IL-2 can be aided to kill and clear the bacterial load within infected cells. Since its depletion is associated with high bacterial load. In addition, we have shown that high levels of TNF-α and low levels of IL-2 are associated with *MTB* growth.

For future research, the inclusion of the chemokines and receptors can enhance the viability of our study. In addition, performing sensitivity analysis on the cytokines and chemokines can provide interesting insight on the dynamics of *MTB* infection.

List of references

[1] Daniel Thomas M. The history of tuberculosis. Respiratory Medicine, 100.11: 1862-1870. 2006.

[2] Alex Sakula. Robert Koch: centenary of the discovery of the tubercle bacillus. The Lancet. 37.4 : 246-251. 1982.

[3] Christoph Gradmann. Robert Koch and the pressures of scientific research: tuberculosis and tuberculin. Medical History. 45.01: 1-32. 2001.

[4] Stefan Kaufmann. Is the development of a new tuberculosis vaccine possible: Nature Medicine. 6.9: 955-960. 2000.

[5] Sebastien Gagneux, et al. Global phylogeography of Mycobacterium tuberculosis and implications for tuberculosis product development:The Lancet Infectious Diseases. 7.5 : 328-337. 2007.

[6] Simeone Marino, et al. A hybrid multi-compartment model of granuloma formation and T cell priming in tuberculosis. Journal of Theoretical Biology. 280.1: 50-62. 2011.

[7] Jennifer Linderman, et al. A multi-scale approach to designing therapeutics for tuberculosis. Integrative Biology. 591-609. 2015.

[8] Simeone Marino, et al. The human immune response to Mycobacterium tuberculosis in lung and lymph node. Elsevier. 463-486. 2003.

[9] Raja Alamelu. Immunology of Tuberculosis. Annual Review of immunology 213-232. 2004.

[10] Teresa Prezzemolo, et al. Functional signatures of human CD4 and CD8T cell responses to Mycobacterium tuberculosis. Frontiers in Immunology. 2014.

[11] Simeone Marino, et al. A multi-scale approach to designing therapeutics for tuberculosis. Integrative Biology., 479-489. 2011.

[12] Stefan Kaufmann, et al. New vaccines for tuberculosis. The Lancet. 591-609. 2010.

[13] Pushpa Jayaraman, et al. TIM3 Mediates Tcell Exhaustion during Mycobacterial Infection. Plos Pathogens. 591-609. 2016.

[14] Janis Wigginton, et al. A Model to Predict Cell-Mediated Immune Regulatory Mechanisms During Human Infection with Mycobacterium tuberculosis. The Journal of Immunology. 591-609. 2001.

[15] Gopalkrishna Sreejit, et al. The ESAT-6 Protein of Mycobacterium tuberculosis interacts with Beta-2-Microglobulin (B2M) Affecting Antigen Presentation Function of Macrophage. Plos Pathogens. 591-609. 2014.

[16] Yoram Louzoun, et al. A mathematical model for pancreatic cancer growth and treatment. Journal of Theoretical Biology. 351:74-82. 2014.

[17] Paola Italiani, et al. From monocytes to M1/M2 macrophages: phenotypical vs. functional differentiation. M1/M2 Macrophages: The Arginine Fork in the Road to Health and Disease. Frontiers in Immunology. 47. 2015.

[18] https://www.rndsystems.com/resources/articles/macrophage-activation 2011.

[19] Fallahi Sichani, et al. A systems biology approach for understanding granuloma formation and function in tuberculosis. Systems biology of tuberculosis. Springer New York. 127-155. 2013.

[20] Juarez Segovia, et al. Identifying control mechanisms of granuloma formation during M. tuberculosis infection using an agent-based model. Journal of theoretical biology. 231.3 : 357-376. 2004.

[21] Judy Day, et al. Modeling the immune rheostat of macrophages in the lung in response to infection. Proceedings of the National Academy of Sciences. PNAS. 106.27 : 11246-11251. 2009.

[22] Bernadette Saunders, et al. Life and death in the granuloma: immunopathology of tuberculosis. Immunology and Cell Biology. 85.2 : 103-111. 2007.

[23] Amanda Mootoo, et al. TNF-alpha in Tuberculosis: A Cytokine with a Split Personality. Inflammation and Allergy-Drug Targets, Formerly Current Drug Targets-Inflammation and Allergy. 8.1 : 53-62. 2009.

[24] Suely Kashino, et al. Guinea pig model of Mycobacterium tuberculosis latent/dormant infection. Microbes and Infection. Elsevier. 10.14 : 1469-1476. 2008.

[25] Chen, Xinchun, et al. CD4+ CD25+ FoxP3+ regulatory T cells suppress Mycobacterium tuberculosis immunity in patients with active disease. Clinical Immunology. 123.1 : 50-59. 2007.

[26] Sharma Monika, et al. Intracellular survival of Mycobacterium tuberculosis in macrophages is modulated by phenotype of the pathogen and immune status of the host. International Journal of Mycobacteriology. 1.2 : 65-74. 2012.

[27] Venkata Ramanarao Parasa, et al. Modeling Mycobacterium tuberculosis early granuloma formation in experimental human lung tissue. Disease Models and Mechanisms. 7.2 : 281-288 2014.

[28] Miranda Silva, et al. The tuberculous granuloma: an unsuccessful host defence mechanism providing a safety shelter for the bacteria?. Clinical and Developmental Immunology. 2012.

[29] Davis Muse, et al. The role of the granuloma in expansion and dissemination of early tuberculous infection. Elsevier. 136.1 : 37-49. 2009.

[30] Neel Gandhi, et al. Extensively drug-resistant tuberculosis as a cause of death in patients co-infected with tuberculosis and HIV in a rural area of South Africa. The Lancet. 368.9547: 1575-1580. 2006.

[31] http://tbfacts.org/tb-tests/. Accessed: November 2016.

[32] Helen Jenkins, et al. Incidence of multidrug-resistant tuberculosis disease in children: systematic review and global estimates. The Lancet. 383.9928 : 1572-1579. 2014.

[33] Charles Janeway, et al. Immunobiology: the immune system in health and disease. Current Biology. 1997.

[34] Lauren Sompayrac, et al. How the immune system works. National Institute of Allergy and Infectious Diseases. 8-15. 2015.

[35] Lauren Sompayrac, et al. How the immune system works. National Institute of Allergy and Infectious Diseases. 5-7. 2015.

[36] Andrea Cooper. Cell mediated immune responses in tuberculosis. Annual review of immunology. 27 :393. 2009.

[37] Davis Muse, et al. The role of the granuloma in expansion and dissemination of early tuberculous infection. Elsevier., 136.1: 37-49. 2009.

[38] Zink A.R, et al. Molecular history of tuberculosis from ancient mummies and skeletons. International Journal of Osteoarchaeology. 17.4 : 380-391. 2007.

[39] David McMurray. Guinea Pig Model of Tuberculosis. American Society for Microbiology. 135-147. 1994.

[40] Global tuberculosis report. World Health Organization. 12-13. 2015.

[41] Global tuberculosis report. World Health Organization. 17-18. 2015.

[42] Global tuberculosis report. World Health Organization. 13-14. 2016.

[43] Daniel Roach, et al. TNF regulates chemokine induction essential for cell recruitment granuloma formation and clearance of mycobacterial infection. The Journal of Immunology. 168.9 : 4620-4627. 2002.

[44] Amanda Mootoo, et al. TNF-alpha in Tuberculosis: A Cytokine with a Split Personality. Inflammation & Allergy-Drug Targets (Formerly Current Drug Targets-Inflammation & Allergy). 8.1 : 53-62. 2009.

[45] Pai Madhukar, et al. New tools and emerging technologies for the diagnosis of tuberculosis: part 2. Active tuberculosis and drug resistance. Expert review of molecular diagnostics 6.3 : 423-432. 2006.

[46] Evelyn Guirado, et al. Modeling the Mycobacterium tuberculosis granuloma-the critical battlefield in host immunity and disease. Frontiers in Immunology. 98.4: 3-4. 2013.

[47] Issar Smith. Mycobacterium tuberculosis pathogenesis and molecular determinants of virulence. Clinical Microbiology Reviews. 16.3 : 463-496. 2003.

[48] Christopher Desjardins, et al. Genomic and functional analyses of Mycobacterium tuberculosis strains implicate ald in D-cycloserine resistance. Nature Genetics. 48.5 : 544-551. 2016.

[49] Gary Winslow, et al. Early T-cell responses in tuberculosis immunity. Immunological Reviews. 225.1 : 284-299. 2008.

[50] Dominic O'hanlon, et al. T cell contributions to the different phases of granuloma formation. Elsevier. 92.1 : 135-142. 2004.

[51] Andrea Cooper, et al. The role of cytokines in the initiation, expansion, and control of cellular immunity to tuberculosis. Immunological Reviews. 226.1 : 191-204. 2008.

[52] Pauline Van den Driessche, et al. Reproduction numbers and sub-threshold endemic equilibria for compartmental models of disease transmission. Mathematical Biosciences. 180.1 : 29-48. 2002.

[53] Ruy Ribeiro, et al. Estimation of the initial viral growth rate and basic reproductive number during acute HIV-1 infection. Journal of Virology. 84.12 : 6096-6102. 2010.

[54] Wu Jing, et al. Multiple cytokine responses in discriminating between active tuberculosis and latent tuberculosis infection. Elsevier. 102 : 68-75. 2017.

[55] Murugesan VS Rajaram, et al. Macrophage immunoregulatory pathways in tuberculosis. Seminars in immunology. Academic Press. 26.6. 2014.

[56] Dirk Schnappinger, et al. Transcriptional adaptation of Mycobacterium tuberculosis within macrophages. Journal of Experimental Medicine. 198.5 : 693-704. 2003.

[57] Michael Lehrke, et al. Inflamed about obesity. Nature Medicine. 10.2 : 126-127. 2004.

[58] David Alleva, et al. Tumor-induced regulation of suppressor macrophage nitric oxide and TNF-alpha production. Role of tumor-derived IL-10, TGF-beta, and prostaglandin E2. The Journal of Immunology. 153.4 : 1674-1686. 1994.

[59] Hannah Volkman, et al. Tuberculous granuloma induction via interaction of a bacterial secreted protein with host epithelium. Science. 327.5964 : 466-469. 2010.

[60] Rishi Vishal Luckheeram, et al. CD4 < sup. Clinical and Developmental Immunology. 2012.

[61] Henk-Jan Van Den Ham, et al. From the two-dimensional Th1 and Th2 phenotypes to high-dimensional models for gene regulation. International Immunology. 20.10 : 1269-1277. 2008.

[62] Carys Kenway-Lynch, et al. Cytokine/Chemokine responses in activated CD4+ and CD8+ T cells isolated from peripheral blood, bone marrow, and axillary lymph nodes during acute simian immunodeficiency virus infection. Journal of Virology. 88.16 : 9442-9457. 2014.

[63] Daniel Barber, et al. Restoring function in exhausted CD8 T cells during chronic viral infection. Nature. 439.7077 : 682-687. 2006.

[64] Gonzalez-Juarrero Mercedes, et al. Temporal and Spatial Arrangement of Lymphocytes within Lung Granulomas Induced by Aerosol Infection with Mycobacterium tuberculosis. Infection and Immunity. 69.3 : 1722-1728. 2001.

[65] JoAnne Flynn, et al. Immunology of tuberculosis. Annual Review of Immunology. 19.1 : 93-129. 2001.

[66] Wang Feng, et al. Mycobacterium tuberculosis-specific TNF-alpha is a potential biomarker for the rapid diagnosis of active tuberculosis disease in Chinese population. Plos. 8.11 : e79431. 2013.

[67] Tim Mosmann, et al. The expanding universe of T-cell subsets: Th1, Th2 and more. Immunology Today. 17.3 : 138-146. 1996.

[68] Lee Segel, et al. The quasi steady state assumption: a case study in perturbation. SIAM Review. 31.3 : 446-477. 1989.

[69] David Russell, et al. Foamy macrophages and the progression of the human TB granuloma. Nature of Immunology. 10.9 : 943. 2009.

[70] Pauline Van den Driessche, et al. Reproduction numbers and sub-threshold endemic equilibria for compartmental models of disease transmission. Mathematical Biosciences. 180.1 : 29-48. 2002.

[71] David Russell. Who puts the tubercle in tuberculosis?. Nature Reviews Microbiology. 5.1 : 39-47. 2007.

[72] Christopher Cambier, et al. Mycobacteria manipulate macrophage recruitment through coordinated use of membrane lipids. Nature. 505.7482 : 218-222. 2014.

[73] Nisheeth Agarwal, et al. Subversion from the Sidelines. Science. 327.5964 : 417-418. 2010.

[74] Harald Wiker, et al. The antigen 85 complex: a major secretion product of Mycobacterium tuberculosis. Microbiological Reviews. 56.4 : 648-661. 1992.

[75] Gesham Magombedze, et al. Latent tuberculosis: models, computational efforts and the pathogens regulatory mechanisms during dormancy. Frontiers in Bioengineering and Biotechnology. 1 : 4. 2013.

[76] Redford P.S, et al. The role of IL-10 in immune regulation during M. tuberculosis infection. Mucosal Immunology. 4.3 : 261-270. 2011.

[77] Gaston Mazandu, et al. Generation and analysis of large-scale data-driven Mycobacterium tuberculosis functional networks for drug target identification. Advances in Bioinformatics. 2011.

[78] Vladimir Yeremeev, et al. Proteins of the Rpf family: immune cell reactivity and vaccination efficacy against tuberculosis in mice. Infection and Immunity. 71.8 : 4789-4794. 2003.

[79] Rustom Antia, et al. A model of non-specific immunity. Journal of Theoretical Biology. 168.2 : 141-150. 1994.

[80] Sushil Kumar Pathak, et al. Direct extracellular interaction between the early secreted antigen ESAT-6 of Mycobacterium tuberculosis and TLR2 inhibits TLR signaling in macrophages. Nature Immunology. 8.6 : 610-618. 2007.

[81] http://www.uniprot.org/uniprot/P61769

[82] Carey Lumeng, et al. Obesity induces a phenotypic switch in adipose tissue macrophage polarization. The Journal of Clinical Investigation. 117.1 : 175-184. 2007.

[83] Alberto Mantovani, et al. Macrophage polarization: tumor-associated macrophages as a paradigm for polarized M2 mononuclear phagocytes. Trends in Immunology. 23.11 : 549-555. 2002.

[84] Cowley Siobhán, et al. CD4+ T cells mediate IFN-gamma-independent control of Mycobacterium tuberculosis infection both in vitro and in vivo. The Journal of Immunology. 171.9 : 4689-4699. 2003.

[85] Zhilan Feng, et al. On the role of variable latent periods in mathematical models for tuberculosis. Journal of Dynamics and Differential Equations, 13.2 : 425-452. 2001.

[86] Lee Jinhee, et al. Macrophage apoptosis in tuberculosis. Yonsei Medical Journal. 50.1 : 1-11. 2009.

[87] Subbarao Sathyavani, et al. Raised venous lactate and markers of intestinal translocation are associated with mortality among in-patients with HIV-associated TB in rural South Africa. Journal of Acquired Immune Deficiency Syndromes. 70.4 : 406. 1999, 2015.

[88] García-Pérez, et al. Internalization of Mycobacterium tuberculosis by macropinocytosis in non-phagocytic cells. Microbial Pathogenesis. 35.2 : 49-55. 2003.

[89] Bansal Shruti, et al. Depolymerase improves gentamicin efficacy during Klebsiella pneumoniae induced murine infection. BMC Infectious Diseases. 14.1 : 456. 2014.

[90] Ying Zhang, et al. New drug candidates and therapeutic targets for tuberculosis therapy. Drug Discovery Today 11.1 : 21-27. 2006.

[91] Gaston Kuzamunu Mazandu, et al. Enhancing drug target identification in Mycobacterium tuberculosis. Tuberculosis: Risk Factors, Drug Resistance and Treatment. Hauppage, NY: NOVA Publishers. 2012

[92] Allen L.J Introduction to mathematical biology. Pearson/Prentice Hall 2007.

[93] Van den Driessche, et al. "Reproduction numbers and sub-threshold endemic equilibria for compartmental models of disease transmission. Mathematical Biosciences. 180.1 : 29-48. 2002.

[94] Gerald Teschl. Ordinary Differential Equations and Dynamical Systems. American Mathematical Society. 140.1 : 49-50. 2012.

[95] Castillo-Chavez, et al. On the computation of R0 and its role on global stability. Mathematical approaches for emerging and reemerging infectious diseases: an introduction. 1:229. 2001.